

Copper(I)-Catalyzed Azide-Alkyne Cycloaddition with Membrane-Bound Lipid Substrates

Kinetics and Effects of Triazole Formation on Lipid
Membranes

Jennifer Beveridge

A thesis presented for the degree of
Master of Science

Department of Chemistry and Biochemistry
Georgia Institute of Technology
May 2015

Copyright ©by Jennifer Marie Beveridge 2015

Copper(I)-Catalyzed Azide-Alkyne Cycloaddition with Membrane-Bound Lipid Substrates

Approved by:

Professor M.G. Finn, Advisor
School of Chemistry and Biochemistry
Georgia Institute of Technology

Professor Nicholas Hud
School of Chemistry and Biochemistry
Georgia Institute of Technology

Professor Alfred Merrill
School of Biology
Georgia Institute of Technology

Date Approved: April 24, 2015

Acknowledgements

I would like to express a gratitude to the numerous people who have helped me and supported me with the writing of this thesis. Firstly, I would like to thank my family for their support throughout my education and without whom, I would not be where I am today. I am also grateful for the support and guidance of my advisor and mentor Professor M.G. Finn. Additionally, I would like to thank Haley Chenot, an undergraduate researcher, for her dedication, as well as for her chemical and programming acumen. I am also thankful for the advice and encouragement from my fellow labmates, including Dr. Michael Baksh, Dr. Roman Valiulin, Dr. Craig McKay, Dr. Srinivas Tekkam, Allison Geoghan, Cody Higginson, Ashley Lockwood, Zhishuai Geng, and Breanne Hamlett.

Contents

List of Tables	vi
List of Figures	vii
List of Abbreviations	xi
Summary	xii
1 Introduction	1
1.1 Introduction to Copper(I)-Catalyzed [3+2] Azide-Alkyne Cycloaddition	1
1.2 Biological Importance of Lipid Membranes	3
1.3 Chemical Reactivity of Membrane-Bound Substrates	3
1.4 [3+2] Azide-Alkyne Cycloaddition with Membrane-Bound Substrates . .	5
2 Synthesis and Characterization of Clickable Lipid-Like Molecules	8
2.1 Overview of Synthetic Strategy	8
2.2 Synthesis of 3-azido-2-oxo-2H-chromen-7-yl-2-(octadecylamino)acetate	9
2.3 Synthetic scheme for N-(prop-2-yn-1-yl)octadecan-1-amine	10
2.4 Synthesis of 6-azido-7-oxo-7,8-dihydronaphthalen-2-yl((3S,8S,9S,10R,13R,14S,17R)-10,13-dimethyl-17-((R)-6-methylheptan-2-yl)-2,3,4,7,8,9,10,11,12,13,14,15,16,17-tetradecahydro-1H-cyclopenta[a]phenanthren-3-yl)carbonate	11
2.5 Synthesis of 7-hydroxy-3-(4-(2-hydroxypropan-2-yl)-1H-1,2,3-triazol-1-yl)-2H-chromen-2-one	12
3 Creation and Characterization of Small Unilamellar Vesicles	13
3.1 Choice of Lipid System	13

3.2	Preparation of Small Unilamellar Vesicles	14
3.3	Copper Catalyzed Azide-Alkyne Cycloaddition of Membrane-Bound Substrates	16
3.4	Characterization of Small Unilamellar Vesicles	17
4	Kinetics with Membrane-Bound Lipid Substrates	19
4.1	Kinetics Experimental	19
4.2	Photobleaching and Quenching for Coumarin-Based Systems and other Experimental Incidentals	20
4.3	Kinetics in Solution	21
4.4	Kinetics with Membrane Bound-Lipid Substrates	24
4.5	Intra-vesicular Reactivity vs. Inter-vesicular Reactivity	27
5	Conclusions and Future Work	31
5.1	In Summary	31
5.2	Looking Forward	32
A	Plate Reader Fluorescence Data	34
	References	44

List of Tables

3.1	Vesicle Types and Composition	15
3.2	Vesicle Characterization	17
4.1	Reactivity of Azidocoumarin and 2-methyl-3-butyn-2-ol in Solution . . .	25
4.2	Reactivity of Membrane Bound Azide and Alkyne	27
4.3	Intra-vesicular vs. Inter-vesicular Reactivity	28

List of Figures

1.1	CuAAC reaction scheme for alkyl and aryl R ¹ and R ²	1
1.2	Catalytic Cycle proposed by Worrell et. al. for CuAAC	2
1.3	Reactivity of Nucleophile-Electrophile Pairs with Fluid Lipid Membranes.	4
1.4	Previously Synthesized Azide and Alkyne Functionalized Lipids by Neef, Gubbens, Gaebler, Smith, and others.	6
2.1	7-hydroxyazidocoumarin exhibits low fluorescence on its own, but when the azide reacts to form a triazole, the resultant product exhibits an intense fluorescence at 476 nm when excited at 404 nm.	9
2.2	Synthetic scheme for an azido-modified lyso-like lipid	9
2.3	Synthetic scheme for an alkyne-modified lyso-like lipid	10
2.4	Synthetic scheme for azidocoumarin-labeled cholesterol.	11
2.5	Synthetic scheme for coumarin triazole.	12
3.1	Observation of Micelle Formation upon Introduction of Artificial Lipids into Egg PC Lipid System	14
3.2	No Micelle Formation Observed upon Introduction of Artificial Lipids into DPPC Lipid System	15
3.3	Fabrication of Small Unilamellar Vesicles	16
3.4	Vesicle Size Pre- and Post-CuAAC	18
3.5	Zeta Potential Pre- and Post-CuAAC	18
4.1	Illustration of Kinetics Experimental Setup	19
4.2	NMR Aromatic Region of Active Azidocoumarin-Based Lipid	20
4.3	NMR Aromatic Region of Photodegraded Azidocoumarin-Based Lipid	20

4.4	Image of Photodegraded (left) and Non-photodegraded (right) Azidocoumarin-Based Lipid in CDCl_3	21
4.5	Kinetic traces for lipid-bound azide substrate undergoing CuAAC. Note the decrease in fluorescence intensity at long times due to photobleaching; the data points showing negative fluorescence are due to a mechanical or software error in the instrument and were ignored to generate Figure 4.6.	22
4.6	Kinetic traces for lipid-bound azide substrate undergoing CuAAC after quenched samples and machine error data points are removed	22
4.7	Initial Kinetics Plot for 7-hydroxy-3-azidocoumarin in Solution	23
4.8	Rate Order Plot for 7-hydroxy-3-azidocoumarin in Solution	23
4.9	Initial Kinetics Plot for 2-methyl-3-butyn-2-ol in Solution	24
4.10	Rate Order Plot for 2-methyl-3-butyn-2-ol in Solution	24
4.11	CuAAC of Membrane Bound Azidocoumarin with Alkyne in Solution Creates an Increase in Fluorescence	25
4.12	Initial Kinetics Plot for Membrane-Bound Azide	25
4.13	Rate Order Plot for Membrane-Bound Azide	25
4.14	CuAAC of Membrane Bound Alkyne with Azidocoumarin in Solution Creates an Increase in Fluorescence	26
4.15	Preliminary Initial Kinetics Plot for Membrane-Bound Alkyne	26
4.16	Rate Order Plot for Membrane-Bound Alkyne	26
4.17	Intravesicular vs. Interventricular Reactivity	27
4.18	Initial Rate of Reaction for Azide and Alkyne Lipids in the Same Vesicle is Concentration Dependent, Suggesting an Inter-vesicular Reaction	28
4.19	Reactive Species in Separate Vesicles Have a Higher Probability of Finding an Adequate Partner Rapidly	29
4.20	Possible routes for the observed reaction of azide-vesicles with alkyne-vesicles to produce triazoles without vesicle aggregation.	30
A.1	Fluorescence evolution for coumarin substrates undergoing CuAAC.	34
A.2	Fluorescence As A Function of Concentration of Coumarin-Triazole	35
A.3	Fluorescence As A Function of Concentration of Coumarin-Triazole (Zoomed to lower concentrations)	35

A.4	Background Fluorescence Traces for Reactions in Solution (Azide). Raw data for Figure 4.7.	36
A.5	Raw Fluorescence Traces for Reactions in Solution (Azide) Raw data for Figure 4.7.	36
A.6	Fluorescence Traces for Reactions in Solution (Azide) with Backgrounds Subtracted. Corresponds to Figure 4.7.	37
A.7	Background Fluorescence Traces for Reactions in Solution (Alkyne). Raw data for Figure 4.9.	37
A.8	Raw Fluorescence Traces for Reactions in Solution (Alkyne) Raw data for Figure 4.9.	38
A.9	Fluorescence Traces for Reactions in Solution (Alkyne) with Backgrounds Subtracted. Corresponds to Figure 4.9.	38
A.10	Background Fluorescence Traces for Reaction with Membrane-Bound Azide. Raw data for Figure 4.12.	39
A.11	Raw Fluorescence Traces for Reactions with Membrane-Bound Azide. Raw data for Figure 4.12.	39
A.12	Fluorescence Traces for Reactions with Membrane-Bound Azide with Background Subtracted. Corresponds to Figure 4.12.	40
A.13	Background Fluorescence Traces for Reaction with Membrane-Bound Alkyne). Raw data for Figure 4.15.	40
A.14	Raw Fluorescence Traces for Reactions with Membrane-Bound Alkyne. Raw data for Figure 4.15.	41
A.15	Fluorescence Traces for Reactions with Membrane-Bound Alkyne with Backgrounds Subtracted. Corresponds to Figure 4.15.	41
A.16	Background Fluorescence Traces for "Intravesicular" Reaction. Raw Data for Figure 4.18 and Table 4.3.	41
A.17	Raw Fluorescence Traces for "Intravesicular" Reaction. Raw Data for Figure 4.18 and Table 4.3.	42
A.18	Fluorescence Traces for "Intravesicular" Reaction with Backgrounds Subtracted. Corresponds to Figure 4.18 and Table 4.3.	42
A.19	Background Fluorescence Traces for Intervesicular Reaction. Raw Data for Table 4.3.	42

A.20 Raw Fluorescence Traces for Interventricular Reaction. Raw Data for Table 4.3.	43
A.21 Fluorescence Traces for Interventricular Reaction with Backgrounds Subtracted. Corresponds to Table 4.3.	43

List of Abbreviations

Abbreviation	Name
CuAAC	Copper(I) Catalyzed Azide-Alkyne Cycloaddition
DMF	N,N-Dimethylformamide
DLS	Dynamic Light Scattering
DMPS	1,2-dimyristoyl-sn-glycero-3-phospho-L-serine
DPPC	1,2-dipalmitoyl-sn-glycero-3-phosphocholine
EtOAc	Ethyl Acetate
FRAP	Fluorescence Recovery After Photobleaching
Hex	Hexanes
KO ^t Bu	Potassium tert-Butoxide
PC	Phosphatidylcholine
SUV	Small Unilamellar Vesicle
THPTA	Tris(3-hydroxypropyltriazolylmethyl)amine

Summary

The bioorthogonal copper(I)-catalyzed azide-alkyne cycloaddition (CuAAC) reaction exhibits complex but well-defined kinetics in aqueous and organic solution for soluble azides, alkynes, and ligand-bound copper(I). The kinetic profile in two dimensions, however, for CuAAC systems within a lipid bilayer membrane, has yet to be defined. The effect of triazole formation with lipid membrane-bound components on membrane properties such as fluidity and permeability is also of interest. Azide- and alkyne-functionalized lysolipids were synthesized and incorporated into non-fluid vesicles, which were then subject to CuAAC. The rate order for membrane-bound lipid substrates in non-fluid vesicles was observed to be comparable to that of the reaction in solution. Reactions between vesicles showed evidence of lipid transfer between non-fluid membranes, which has not been previously reported. For intervesicular and intravesicular reactions in non-fluid membranes, the observed reactivity was found to be opposite that of previously published reactions between nucleophiles and electrophiles in fluid lipid systems. Applications of this work include the potential for novel symmetric membrane leaflet labeling, bioorthogonal manipulation of cell and tissue function, and the creation of membranes with precisely controlled properties that may not be available in naturally-occurring membranes.

Chapter 1

Introduction

Beveridge, J.M., Finn, M.G.

1.1 Introduction to Copper(I)-Catalyzed [3+2] Azide-Alkyne Cycloaddition

Copper(I)-Catalyzed Azide-Alkyne Cycloaddition (CuAAC) is a regioselective and bioorthogonal reaction through which an azide and a terminal alkyne form a 1,4-disubstituted-1,2,3-triazole when in the presence of a copper(I) catalyst and copper(I)-binding ligand, as shown in Figure 1.1.¹

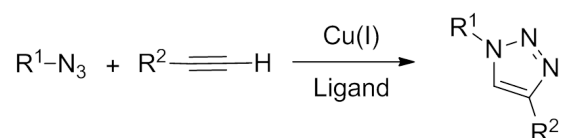


Figure 1.1: CuAAC reaction scheme for alkyl and aryl R¹ and R²

This reaction is wide in scope, meaning it is compatible with a large number of other functional groups, and is tolerant to both aqueous and organic solvents.^{1,2} The kinetics of this reaction in the solution phase, are well-defined. With excess copper, the reaction exhibits first order kinetics with respect to azide and between

¹Rostovtsev, V.V., Green, L.G., Fokin, V.V., Sharpless, K.B. A Stepwise Huisgen Cycloaddition Process: Copper (I)-Catalyzed Regioselective Ligation of Azides and Terminal Alkynes. *Angew. Chem. Int. Ed.* 41, 2596-2599, doi: 10.1002/1521-3773(20020715)41:14<2596::AID-ANIE2596>3.0.CO;2-4 (2002).

²Kolb, H.C., Finn, M.G., Sharpless, K.B. Click Chemistry: Diverse Chemical Function from a Few Good Reactions. *Angew. Chem. Int. Ed.* 40, 11, 2004-2021. doi: 10.1002/1521-3773(20010601)40:11<2004::AID-ANIE2004>3.0.CO;2-5 (2001).

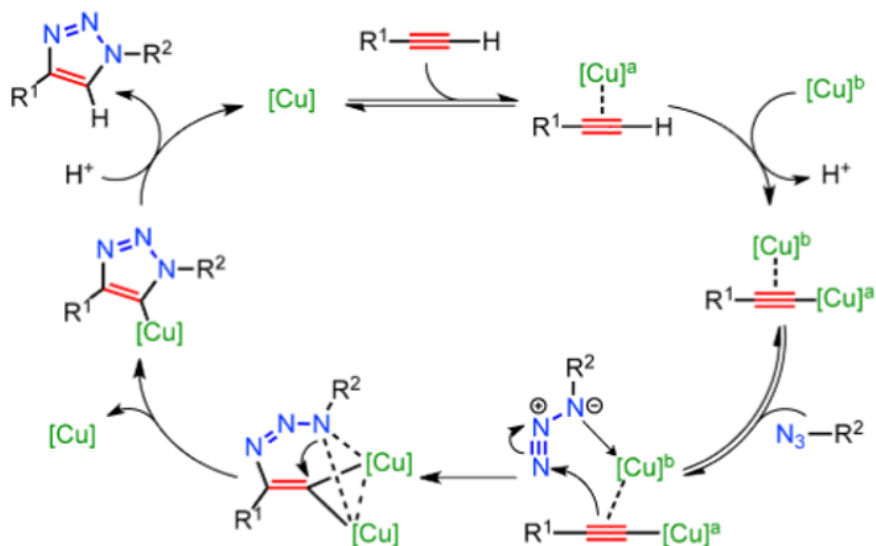


Figure 1.2: Catalytic Cycle proposed by Worrell et. al. for CuAAC

first and second order kinetics with respect to alkyne. With catalytic copper, the system displays second order kinetics with respect to copper.³ Though the mechanism for CuAAC is believed to be somewhat understood for soluble reactants as seen in Figure 1.2,⁴ the reaction between azide and alkyne held in a two-dimensional matrix such as the lipid bilayer may not necessarily proceed via the same mechanism, or may be inhibited by the geometrical or dynamic limitations of membranes.

Fluid lipid bilayers allow for true two-dimensional reactivity because lipids are able to diffuse throughout the membrane within the same leaflet,⁵ whereas with solid, non-membrane supports, the substrates are tethered to the support and the system lacks movement parallel to the support surface.⁶

³Rodionov, V.O., Fokin, V.V., Finn M.G.. Mechanism of the Ligand-Free Cu(I)-Catalyzed Azide-Alkyne Cycloaddition Reaction. *Angew. Chem. Int. Ed.* 44, 2210-2215, doi: 10.1002/anie.200461496 (2005).

⁴Worrell, B.T., Malik, J.A., Fokin, V.V. Direct Evidence of a Dinuclear Copper Intermediate in Cu(I)-Catalyzed Azide-Alkyne Cycloadditions. *Science*, 340, 6131, 457-460, doi: 10.1126/science.1229506 (2013).

⁵O'Leary, T.J. Lateral Diffusion of Lipids in Complex Biological Membranes. *Proc. Natl. Acad. Sci.* 84, 429-433 (1987).

⁶Hodge, P. Polymer-supported Organic Reactions: What Takes Place in the Beads? *Chem. Soc. Rev.* 26, 417-424, doi: 10.1039/CS9972600417 (1997).

1.2 Biological Importance of Lipid Membranes

Lipids self-assemble in aqueous solution to form noncovalently arranged structures, with the polar hydrophilic headgroups facing outward toward the aqueous media and the nonpolar, hydrophobic tails segregated from the aqueous environment, thereby minimizing the hydrocarbon-water contact and lowering the free energy of the system.⁷ This self-assembly is dictated by both the hydrophobic forces that drive the isolation of the hydrocarbon chains and the ionic and/or steric repulsion of the polar headgroups from one another. The type of structure (vesicles, micelles, flat bilayers) formed by lipids in aqueous solutions depends on headgroup area, chain volume, and chain length.⁸ Lipid bilayers, of course, play a vital role in cell organization and compartmentalization, making up the cellular and organelle membranes, and are involved in trafficking and regulating the movement of ions and organic molecules.⁹ Biological membranes also contain cholesterol, membrane-associated proteins, and glycosylated lipids and proteins which work together to execute membrane-related processes.¹⁰

1.3 Chemical Reactivity of Membrane-Bound Substrates

Studies of the dynamic behavior of membranes has led to the proposal of lipid microdomains, in which lipids phase separate, with portions of the membrane exhibiting characteristics of both liquid- and gel-phase lipids.¹¹ This dynamic behavior has prompted much research into the formation and role of lipid microdomains in cellular processes, and suggests a need for further studies into membrane be-

⁷Ruckenstein, E., Nagarajan, R. Thermodynamics of Amphiphilic Aggregation into Micelles and Vesicles. *Micellization, Solubilization, and Microemulsions*, Vol. 1, Plenum Press: New York (1977).

⁸Lindblom, G., Wennerström, H. Amphiphile Diffusion in Model Membrane Systems Studied by Pulsed NMR. *Biophys. Chem.* 6, 2, 167-171 (1977).

⁹Alberts, B., Johnson, A., Lewis, J., Raff, M., Roberts, K., Walter, P. *Molecular Biology of the Cell*, 5th Ed., Garland Science: New York (2007).

¹⁰Lillemeier, B.F., Pfeiffer, J.R., Surviladze, Z., Wilson, B.S., Davis, M.M. Plasma Membrane-Associated Proteins are Clustered into Islands Attached to the Cytoskeleton. *Proc. Nat. Acad. Sci.* 103, 50, 18992-18997, doi: 10.1073/pnas.0609009103 (2006).

¹¹Simons, K., Vaz, W.L.C. Model Systems, Lipid Rafts, and Cell Membranes. *Annu. Rev. Biophys. Biomol. Struct.* 33, 269-295, doi: 10.1146/annurev.biophys.32.110601.141803 (2004).

havior in both liquid- and gel-phases,^{12,13} because these microdomains are vital chemically reactive sites within the membrane.^{14,15} Lipid involvement in the organization of these microdomains is particularly relevant for cell signalling and communication.¹⁶

Lipids and interactions between lipids have been documented to play a large role in controlling neuronal communication and behavior,¹⁷ which suggests the need for understanding reactivity between lipid membranes. Reactivity between membrane-bound substrates in two independent vesicles, as well as within the same vesicle, have been evaluated by Menger using a cholesterol-bound hydroxamate nucleophile and a p-nitrophenyl ester electrophile by Menger. For the fluid lipid system employed, it was observed that intravesicular reactions proceed faster than solution-solution reactions and solution-vesicle reactions, with intervesicular reactions proceeding the most slowly, as shown in Figure 1.3.¹⁸

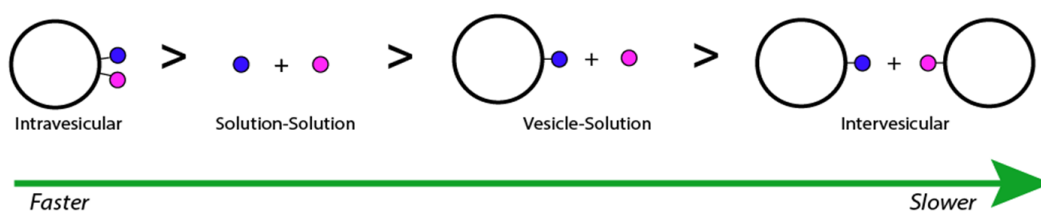


Figure 1.3: Reactivity of Nucleophile-Electrophile Pairs with Fluid Lipid Membranes.

When the same cholesterol-bound hydroxamate nucleophile was reacted with a lipid analogue of a quinolium ester, collisions between vesicles led to a transfer of the the lipid electrophile from one vesicle to another, which was then followed by

¹²Eggeling, C., et al. Direct Observation of the Nanoscale Dynamics of Membrane Lipids in a Living Cell. *Nature* 457, 1159-1162, doi: 10.1038/nature07596 (2009).

¹³Pierce, S.K. Lipid Rafts and B-cell Activation. *Nat. Rev. Immun.* 2, 96-105, doi: 10.1038/nri726 (2002).

¹⁴Radhakrishnan, A., Anderson, T.G., McConnell, H.M. Condensed Complexes, Rafts, and the Chemical Activity of Cholesterol in Membranes. *Proc. Natl. Acad. Sci.* 97, 23, 12422-12427, doi: 10.1073/pnas.220418097 (2000).

¹⁵Young, R.M., Holowka, D., Baird, B. A Lipid Raft Environment Enhances Lyn Kinase Activity by Protecting the Active Site Tyrosine from Dephosphorylation. *J. Bio. Chem.* 278, 20746-20752, doi: 10.1074/jbc.M211402200 (2003).

¹⁶Fessler, M.B., Parks, J.S. Intracellular Lipid Flux and membrane Microdomains as Organizing Principles in Inflammatory Cell Signalling. *J. Immunol.* 187, 1529-1535, doi: 10.4049/jimmunol.1100253 (2011).

¹⁷Di Paolo, G., Moskowitz, H.S., Gipson, K., Wenk, M.R., Voronov, S., Obayashi, M., Ravell, R., Fitzsimonds, R.M., Ryan, T.A., De Camilli, P. Impaired PtdIns(4,5)P₂ Synthesis In Nerve Terminals Produces Defects in Synaptic Vesicle Trafficking. *Nature* 431, 415-422, doi: 10.1038/nature02896 (2004).

¹⁸Menger, F.M., Azov, V.A. Cytomimetic Modeling in Which One Phospholipid Liposome Chemically Attacks Another. *J. Am. Chem. Soc.* 122, 6492-6493, doi: 10.1021/ja000504x (2000).

a rapid intravesicular reaction.¹⁹ This observation of lipid transfer without assistance from proteins to facilitate exchange was not the first of its kind. Spontaneous lipid transfer, via monomer diffusion or transient contact, has been observed in many model fluid membrane systems with both phospholipids and lysolipids.^{20,21} The observed rate of cholesterol and lipid transfer, however, varies greatly depending on the lipid. It has been reported to be as fast as an exchange half time of 2.3 hours for [4-¹⁴C]cholesterol or as slow as 48 hours for 1-palmitoyl-2-oleoyl [1-¹⁴C] phosphatidylcholine.²² Membranes, therefore, are two-dimensional systems of great biological importance that exhibit variable fluidity and are chemically addressible.

1.4 [3+2] Azide-Alkyne Cycloaddition with Membrane-Bound Substrates

Lipids are biologically vital molecules, and interest in studying lipid membrane dynamic behavior makes the ability to observe lipid membrane behavior, alter membrane composition, and selectively target lipid membranes useful. Some research has been done toward these aims. Neef and others created strained cyclooctyne-based lipids, able to undergo cycloaddition to form 1,2,3-triazoles with suitable azide fluorophores in live cells without copper;²³ however, these strained cyclooctyne systems are sterically bulky and may perturb the dynamics of lipid system being observed. Alternatively, several researchers have made lipid analogues compatible with CuAAC. The ability to perform CuAAC with lipid membrane-bound substrates provides a platform for studying the reaction in a two-dimensional system, a tool for symmetric membrane labeling of lipid membrane leaflets, and a

¹⁹Menger, F.M., Caran, K.L, Seredyuk, V.A. Chemical Reaction between Colliding Vesicles. *Angew. Chem. Int. Ed.* 40, 20, 3905-3907, doi: 10.1002/1521-3773(20011015)40:20;3905::AID-ANIE3905;3.0.CO;2-B (2001).

²⁰Sleight, R.G. Intracellular Lipid Transport in Eukaryotes. *Ann. Rev. Physiol.* 49, 193-208, doi: 10.1146/annurev.ph.49.030187.001205 (1987).

²¹Needham, D., Zhelev, D.V. Lysolipid Exchange with Lipid Vesicle Membranes. *Ann. Biomed. Eng.* 23, 287-298, doi: 10.1007/BF02584429 (1995).

²²McLean, L.R., Phillips, M.C. Mechanism of Cholesterol and PHosphatidylcholine Exchange or Transfer between Unilamellar Vesicles. *Biochemistry* 20, 10, 2893-2900, doi: 10.1021/bi00513a028 (1981).

²³Neef, A.B., Schultz, C. Selective Fluorescence Labeling of Lipids in Living Cells. *Angew. Chem. Int. Ed.* 48, 1498-1500, doi: 10.1002/anie.200805507 (2009).

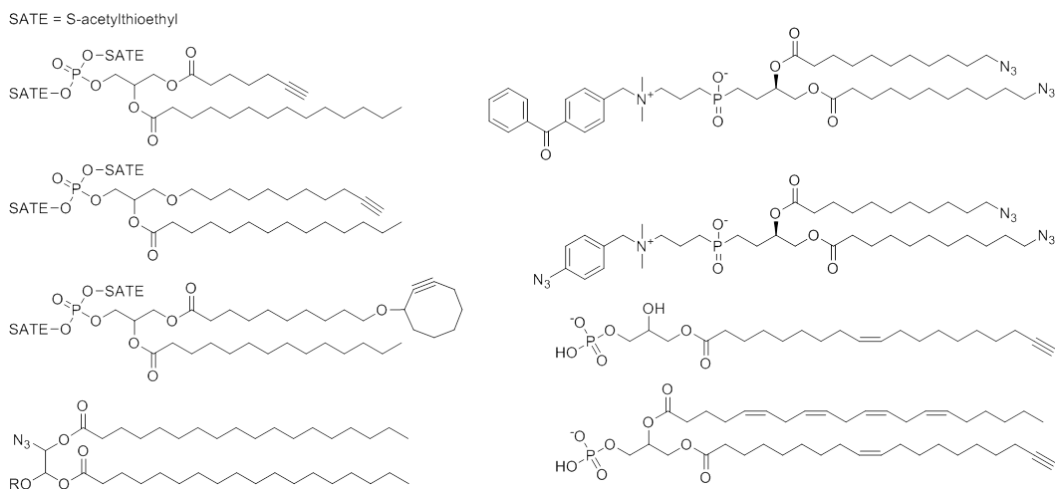


Figure 1.4: Previously Synthesized Azide and Alkyne Functionalized Lipids by Neef, Gubbens, Gaebler, Smith, and others.

means for targeting membranes directly. CuAAC-capable lipids include the azide tail-modified phosphatidylcholine analogs created by Gubbens *et al.*,²⁴ the alkyne tail-modified phospholipid created by Gaebler *et al.*²⁵ and Neef and Schultz,²³ the azide head-modified lipid analogue from Smith *et al.*,²⁶ (see Figure 1.4) and the commercially available Pac FA GalCer from Avanti which features a alkyne modified tail, as well as DSPE-PEG(2000) that features a polyethylene glycol linker between lipid and azide.

Of these, the commercially available azide and alkyne modified lipid analogues are costly or place the azide functional group at a great distance from the lipid bilayer, or buried deep within the membrane. The latter may not be ideal for studying reaction kinetics for CuAAC at the membrane-water interface as reaction participants require access to the other reactive species. The synthetically accessible lipids described above can, at times, provide the functionality in a location as desired, yet the routes to these synthetic targets are arduous, with some low yielding steps. It is desired, therefore, to have synthetically accessible azide and alkyne functionalized lipids by which membrane dynamics can be observed.

²⁴Gubbens, J. *et al.* Photocrosslinking and Click Chemistry Enable the Specific Detection of Proteins Interacting with Phospholipids at the Membrane Interface. *Chemistry & Biology* 16, 3-14, doi: 10.1016/j.chembiol.2008.11.009 (2009).

²⁵Gaebler, A. *et al.* Alkyne Lipids as Substrates for Click Chemistry-Based in vitro Enzymatic Assays. *J Lipid Res.* 54, 8, 2282-2290, doi: 10.1194/jlr.D038653 (2013).

²⁶Smith, M.D. *et al.* Synthesis and Convenient Functionalization of Azide-Labeled Diacylglycerol Analogues for Modular Access to Biologically Active Lipid Probes. *Bioconjugate Chem.* 19, 9, 1855-1863, doi: 10.1021/bc/800102 (2008).

It is also desirable to create a platform for observing membrane kinetics in two-dimensions, and for observing the effects of triazole formation on lipid membranes with membrane-bound CuAAC substrates. This work seeks to create azide and alkyne functionalized lipids via relatively facile synthetic means and will use them to observe membrane kinetics and the effect of triazole formation on the lipid membrane. In the following chapter, the synthetic methods to create the azide and alkyne functionalized lipids will be described.

Chapter 2

Synthesis and Characterization of Clickable Lipid-Like Molecules

Beveridge, J.M., Chenot, H.M., Finn, M.G.

2.1 Overview of Synthetic Strategy

As an alternative to these restrictive synthetic and costly commercially available azide and alkyne modified lipid analogues, we developed more facile synthetic options by designing lyso-like lipid analogues. To promote the kinetic study of their reactions, 7-hydroxy-3-azidocoumarin ($\lambda_{ex} = 404$ nm, $\lambda_{em} = 476$ nm) was used. The fluorescence of this compound is quenched, but conversion of the azide group to the triazole induces relatively strong fluorescence, as seen in Figure 2.1.¹ Attachment of a linker to the hydroxyl group changes, but does not abrogate this convenient activity. Therefore, this fluorophore was incorporated into our synthetic designs as an azide source for each azide modified lipid analogue.

Cholesterol-based lipids have also been used to study reactions between lipid bilayers and have been instrumental in assessing reactivity for interliposomal reactions.² As such, cholesterol derivatives were also created for incorporation into lipid membranes.

¹Sivakumar, K., Xie, F., Cash, B.M., Long, S., Barnhill, H.N., Wang, Q. A fluorogenic 1,3-dipolar cycloaddition reaction of 3-azidocoumarins and acetylenes. *Org. Lett.* 6, 4603-4606, doi:10.1021/ol047955x (2004).

²Menger, F.M., Azov, V.A. Cytomimetic Modeling in Which One Phospholipid Liposome Chemically Attacks Another. *J. Am. Chem. Soc.*, 122, 6492-6493, doi: 10.1021/ja000504x (2000).

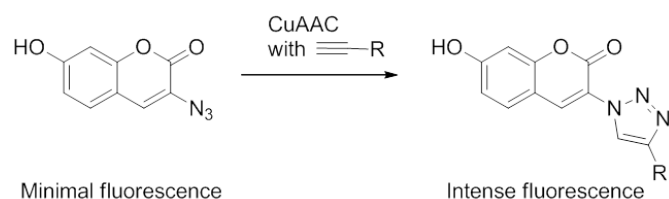


Figure 2.1: 7-hydroxyazidocoumarin exhibits low fluorescence on its own, but when the azide reacts to form a triazole, the resultant product exhibits an intense fluorescence at 476 nm when excited at 404 nm.

The syntheses described herein were not optimized for yield, but rather were required to produce only small amounts of materials for use. All reagents and materials used were obtained commercial sources and were used without further purification, unless otherwise noted.

2.2 Synthesis of 3-azido-2-oxo-2H-chromen-7-yl-2-(octadecylamino)acetate

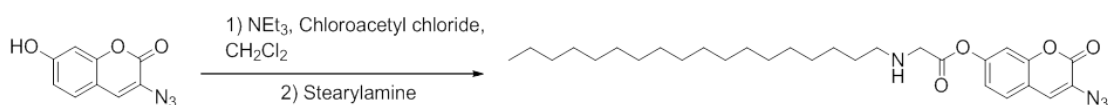


Figure 2.2: Synthetic scheme for an azido-modified lyso-like lipid

7-hydroxy-3-azidocoumarin was synthesized as described by Sivakumar et al.¹ 7-hydroxy-3-azidocoumarin (20 mg, 0.098 mmol, 1 equiv.) and triethylamine (41 μL , 0.3 mmol, 3 equiv.) were stirred in dichloromethane at room temperature in the dark for 5 minutes before chloroacetyl chloride (16 μL , 0.196 mmol, 2 equiv.) was added. This was stirred without light for 10 minutes, at which point stearylamine (53 mg, 0.196 mmol, 2 equiv.) was added. This was stirred for 1 hour at room temperature and purified by medium-pressure chromatography over silica gel (Biotage) with hexane/ethyl acetate gradient ($R_f = 0.28$ for 1:5 EtOAc/Hex). The product (Figure 2.2), obtained as a yellow solid with 13% yield, was extremely photosensitive, especially when dissolved in chloroform.

¹H-NMR (CDCl_3 , 500 MHz): δ (ppm) 0.91 (t, 3H, $J = 7$ Hz), 1.28 (m, 24H), 1.58 (t, 2H, $J = 7$ Hz), 3.33 (q, 2H, $J = 7$ Hz), 4.09 (s, 2H), 4.36 (s, 1H), 6.62 (s,

1H), 6.58 (m, 1H), 7.19 (s, 1H), 7.32 (d, 1H, J= 8 Hz). IR (cm⁻¹): 3289 (secondary amine), 2138 (azide), 1697 (carbonyl), 1642 (carbonyl).

2.3 Synthetic scheme for N-(prop-2-yn-1-yl)octadecan-1-amine

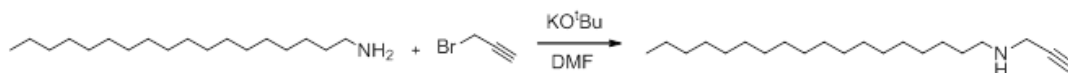


Figure 2.3: Synthetic scheme for an alkyne-modified lyso-like lipid

Stearylamine (50 mg, 0.186 mmol, 1 equiv.) and potassium tert-butoxide (62 mg, 0.557 mmol, 3 equiv.) were combined in DMF (8 mL). The system was purged with nitrogen and heated to 40 °C. Propargyl bromide (18 μ L, 0.204 mmol, 1.1 equiv) was added and the solution was stirred overnight at 40 °C. The reaction was quenched with water and extracted with dichloromethane. The solution was dried over sodium sulfate. Solvent was removed by rotary evaporation with toluene azeotrope to yield a yellow powder and the compound was purified via flash chromatography over silica gel with a hexane/ethyl acetate gradient (R_f = 0.46 for 1:1 EtOAc/Hex). The product (Figure 2.3) was obtained with 56% yield.

¹H-NMR (CDCl₃, 500 MHz): δ (ppm) 0.90 (t, 3H, J = 7 Hz), 1.28 (m, 26H), 1.53 (p, 2H, J= 7 Hz), 2.28 (t, 1H, J= 2 Hz), 2.60 (t, 2H, J= 7 Hz), 3.51 (d, 2H, J = 2 Hz). ¹³C-NMR (CDCl₃, 500 MHz) δ (ppm) 13.94, 22.52, 26.94, 27.11, 29.19, 31.75, 41.87, 52.84, 73.40. Mass Spec: (M + K⁺) 346.50. IR (cm⁻¹): 3290 (alkyne), 3120 (secondary amine), and 2120 (terminal alkyne).

2.4 Synthesis of 6-azido-7-oxo-7,8-dihydronaphthalen-2-yl ((3S,8S,9S,10R,13R,14S,17R)-10,13-dimethyl-17-((R)-6-methylheptan-2-yl)-2,3,4,7,8,9,10,11,12,13,14,15,16,17-tetradecahydro-1H-cyclopenta[a]phenanthren-3-yl) carbonate

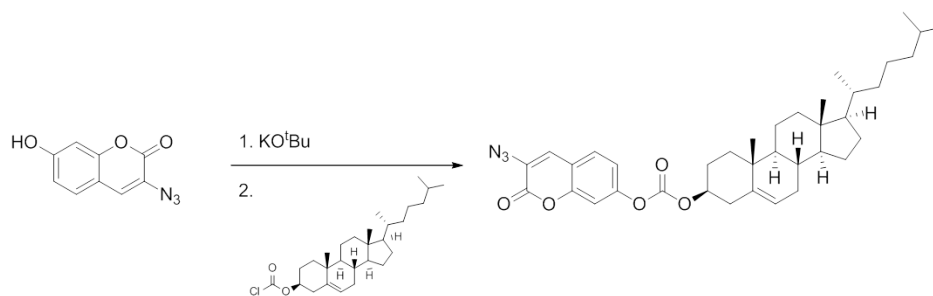


Figure 2.4: Synthetic scheme for azidocoumarin-labeled cholesterol.

7-hydroxy-3-azidocoumarin was synthesized as described by Sivakumar et al.^{??} and dissolved in dichloromethane. Potassium tertbutoxide (15 mg, 0.13 mmol, 1.5 equiv.) was added and the solution was stirred under nitrogen at room temperature. Chloesteryl chloroformate (40 mg, 0.09 mmol, 1 equiv.) was dissolved in dry dichloromethane and stirred overnight. Solvent was removed by rotary evaporation and purified via silica gel column with a hexane/ethyl acetate gradient. (R_f= 0.79 for 1:5 EtOAc/Hex). The product (Figure 2.4), a yellow powder, was obtained with 29% yield.

¹H-NMR (CDCl₃, 500 MHz): δ (ppm) 0.69 (s, 3H), 0.92 (d, 3H, J= 7Hz), 0.97-1.57(m), 1.71-2.02 (m) 2.49(m, 2H), 4.61(septet, 1H, 5 Hz), 5.43 (doublet, 1H, J= 5 Hz), 7.16 (doublet of doublets, 1H, J= 2, 9 Hz), 7.20(s, 1H), 7.25 (d, 1H, J= 2Hz), 7.43 (d, 1H, J=9 Hz).

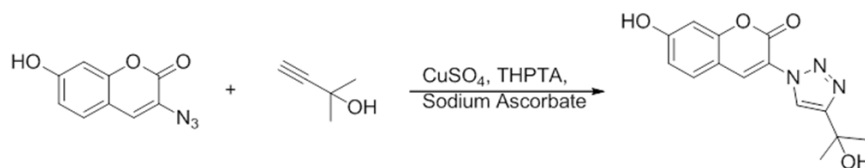


Figure 2.5: Synthetic scheme for coumarin triazole.

2.5 Synthesis of 7-hydroxy-3-(4-(2-hydroxypropan-2-yl)-1H-1,2,3-triazol-1-yl)-2H-chromen-2-one

7-hydroxy-3-azidocoumarin was synthesized as described by Sivakumar et al.^{??} and was mixed (40 mg, 0.20 mmol, 1 equiv.) in water (10 mL) with 2-methyl-3-butyn-2-ol (57 μ L, 0.59 mmol, 3 equiv.), copper(II) sulfate (3 mg, 0.02 mmol, 0.1 equiv.), and THPTA (43 mg, 0.10 mmol, 0.5 equiv.). To this was added sodium ascorbate (39 mg, 0.2 mmol, 1 equiv.), and the solution was stirred at room temperature for 3 hours. Product was extracted with ethyl acetate, washing with water thrice. Solvent was removed by rotary evaporation and further dried by lyophilizer. (Rf=0.10 for 1:1 EtOAc/Hex). The product, a brown powder was obtained in 90% yield.

¹H-NMR (d₄-methanol, 500 MHz): δ (ppm) 1.31 (s, 6H), 3.59 (s, 1H), 4.55 (s, 1H), 6.85 (d, 1H, J=2 Hz), 6.92 (d of d, 1H, J=2, 9 Hz), 7.67 (d, 1H, J= 9 Hz), 8.45 (s, 1H), 8.51 (s, 1H). IR (cm⁻¹): 3345 (alcohol), 1709 (carbonyl), 1604 (alkene), 1252, 1150, 1120 (C-O stretch).

Chapter 3

Creation and Characterization of Small Unilamellar Vesicles

Beveridge, J.M., Baksh, M.M., Chenot, H.M., Finn, M.G.

3.1 Choice of Lipid System

When considering lipid systems with which to evaluate CuAAC kinetics, many platforms are available. We small unilamellar vesicles (SUVs), approximately 75 nm in diameter) for their relatively facile preparation and their consistency with respect to composition and size distribution, relative to larger vesicles, which are usually subject to greater variability in properties.

Initially, we attempted to introduce our artificial lipids into a relatively fluid lipid system comprised of *L-alpha*-phosphatidylcholine (Egg PC) and 1,2-dimyristoyl-sn-glycero-3-phospho-L-serine (DMPS), which are both fairly inexpensive and easy to use for vesicle formation; however, these experiments resulted in the formation of micelles, in addition to vesicles, characterized by average radii of approximately 10 nm as observed by dynamic light scattering (DLS) (Figure 3.1). Note that as smaller objects are less sensitively detected by DLS, the observed distribution indicates a significant population of micelles in these samples.

Experiments performed in micelles would be expected to be subject to aggregation effects rather than by distribution of reactants in "two-dimensional" bilayers.

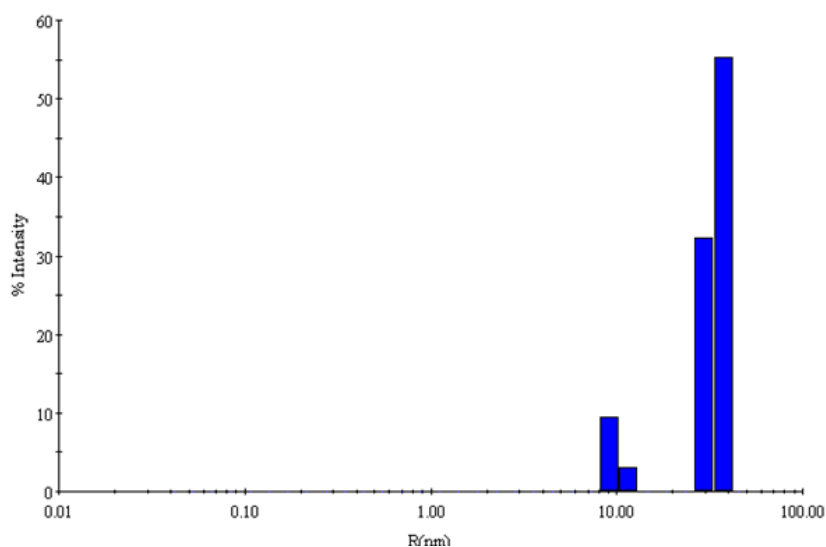


Figure 3.1: Observation of Micelle Formation upon Introduction of Artificial Lipids into Egg PC Lipid System

This type of phase separation and segregation has been observed in other lipid systems^{1,2} and was resolved by creating a more uniform lipid system with a less fluid lipid, 1,2-dipalmitoyl-sn-glycero-3-phosphatidylcholine (DPPC). Vesicles formed from a mixture of DPPC and the synthetic lyso-like lipids described in Chapter 2 showed no evidence of micellar formation (Figure 3.2).

3.2 Preparation of Small Unilamellar Vesicles

Small unilamellar vesicles were prepared similar to the method described by Abramson, Katzman, and Gregor.³ The previously described lyso-like lipids were dissolved in chloroform and mixed with 1,2-dipalmitoyl-sn-glycero-3-phosphocholine (DPPC, Avanti Polar Lipids) and stearylamine such that DPPC made up 99% of the overall lipid concentration and the synthesized lipids and stearylamine made up 1% of the total lipid concentration. In instances where synthesized azide, alkyne, and copper-binding ligand were all used in the same vesicle, no stearylamine was

¹Haluska, C.K., Baptista, M.S., Fernandes, A.U., Schroder, A.P., Marques, C.M., Itri, R. Photo-activated Phase Separation in Giant Vesicles Made from Different Lipid Mixtures. *Biochim. Biophys. Acta* 1818, 3, 666-672, doi: 10.1016/j.bbame.2011.11.025 (2011).

²Johnsson, M., Edwards, K. Liposomes, Disks, and Spherical Micelles: Aggregate Structure in Mixtures of Gel Phase Phosphatidylcholines and Poly(Ethylene Glycol)-Phospholipids. *Biophys. J.* 85, 6, 3839-3847, doi: 10.1016/S0006-3495(03)74798-5 (2003).

³Abramson, M. B., Katzman, R. & Gregor, H. P. Aqueous Dispersions of Phosphatidylserine: Ionic Properties. *J. Biol. Chem.* 239, 70-76 (1964).

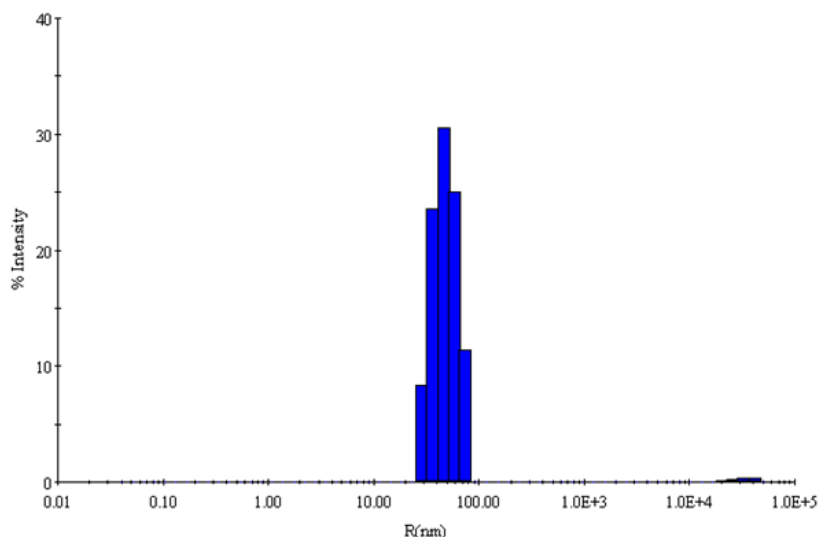
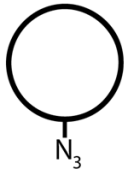
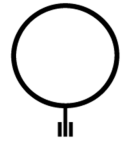
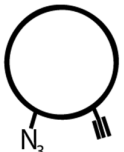


Figure 3.2: No Micelle Formation Observed upon Introduction of Artificial Lipids into DPPC Lipid System

added. When synthesized azide and alkyne were used but the copper-binding ligand was not lipid-bound, the molar ratio that the copper-binding ligand would have comprised was replaced by an equivalent molar ratio of stearylamine. Similarly, in each instance where a vesicle was created to be lacking azide, alkyne, or copper-binding ligand, the molar ratio of the lacking component was replaced with an equivalent molar ratio of stearylamine for consistent lyso-lipid composition between samples. Precise lipid compositions are detailed in Table 3.1.

Table 3.1: Vesicle Types and Composition

Vesicle Type	[DPPC] (mM)	[Azide-Lipid] (μM)	[Alkyne-Lipid] (μM)	[Stearylamine] (μM)
	1.7	48	0.0	53
	1.7	0.0	48	53
	1.7	48	48	5.0

Vesicle creation is depicted in Figure 3.3. Lipids were mixed in chloroform as

described above, and solvent was removed by evaporation in a round-bottom flask to form a thin lipid film. The lipids were rehydrated in a 0.2 M pH 7 sodium phosphate buffer overnight at 4 °C and then warmed gently with heating from a heat gun until fully rehydrated as determined by visual inspection. They were then sonicated with a probe tip sonicator under inert atmosphere and centrifuged at 160,000 x g for 2 hours. The top 20 μ L was removed carefully with a pipette and discarded. The remainder of the supernatant was isolated and used within 24 hours for experimentation.

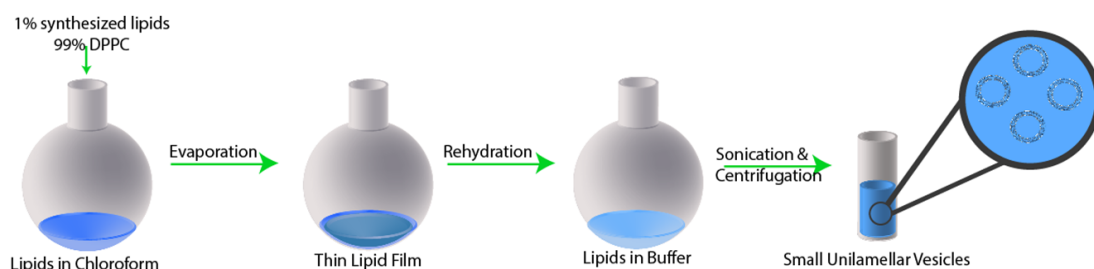


Figure 3.3: Fabrication of Small Unilamellar Vesicles

Thus, relatively uniform vesicles were created with azide- and alkyne-functionalized lipids doped in at specific concentrations to a primarily DPPC membrane, to be used further experimentation.

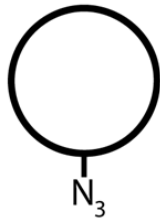
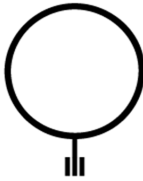
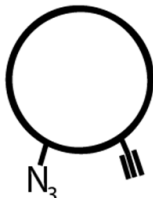
3.3 Copper Catalyzed Azide-Alkyne Cycloaddition of Membrane-Bound Substrates

CuAAC was carried out by mixing equal volumes of azide, alkyne, THPTA, copper(II) sulfate, and sodium ascorbate stock solutions. When one of the reaction substrates was vesicle bound, the concentrations used for the membrane-bound component were those as prepared in the lipid preparations described above. Otherwise, default stock concentrations were as follows: 200 μ M azidocoumarin, 1.9 mM 2-methyl-3-butyn-2-ol, 57 μ M copper(II) sulfate, 300 μ M THPTA, and 13 mM sodium ascorbate. The final concentrations of each in the reaction solutions are as follows: 40 μ M azidocoumarin, 370 μ L 2-methyl-3-butyn-2-ol, 12 μ M copper(II) sulfate, 60 μ M tris(3-hydroxypropyltriazolylmethyl)amine (THPTA), and 2.5 mM sodium ascorbate.

3.4 Characterization of Small Unilamellar Vesicles

Vesicles were characterized by the average of eight DLS measurements and three Zeta Potential measurements for each sample, both pre- and post-CuAAC. In general, vesicles were relatively uniform in size and typically ranged from 30 to 45 nm in radius, depending on the artificial lipid. The vesicles tended to be slightly positively charged, as evaluated by Zeta Potential.

Table 3.2: Vesicle Characterization

Vesicle Type	Radius (nm)	Zeta Potential (mV)
	40.3 ± 10.1	4.06 ± 0.25
	33.0 ± 5.8	5.27 ± 0.09
	32.6 ± 6.0	5.13 ± 0.35

With non-fluid lipids in gel-phase (with experiments performed at room temperature) and with the long octadecyl chains anchoring the synthetic lipids to the membrane, it was anticipated that DLS would show an increase in vesicle size upon triazole formation via CuAAC, due to vesicle aggregation. This, however, was not the case.

The lack of vesicle size change (Figure 3.4), coupled with an increase in fluorescence upon triazole formation, as will be detailed next chapter, suggests a lipid transfer from one vesicle to another, similar to that observed by Menger.⁴ To this

⁴Menger, F.M., Caran, K.L., Seredyuk, V.A. Chemical Reaction between Colliding Vesicles. *Angew. Chem. Int. Ed.* 40, 20, 3905-3907, doi: 10.1002/1521-3773(20011015)40:20<3905::AID-ANIE3905>3.0.CO;2-B (2001).

author's knowledge, this is the first such report of lipid transfer between non-fluid vesicles or between lipid bilayers in gel phase.

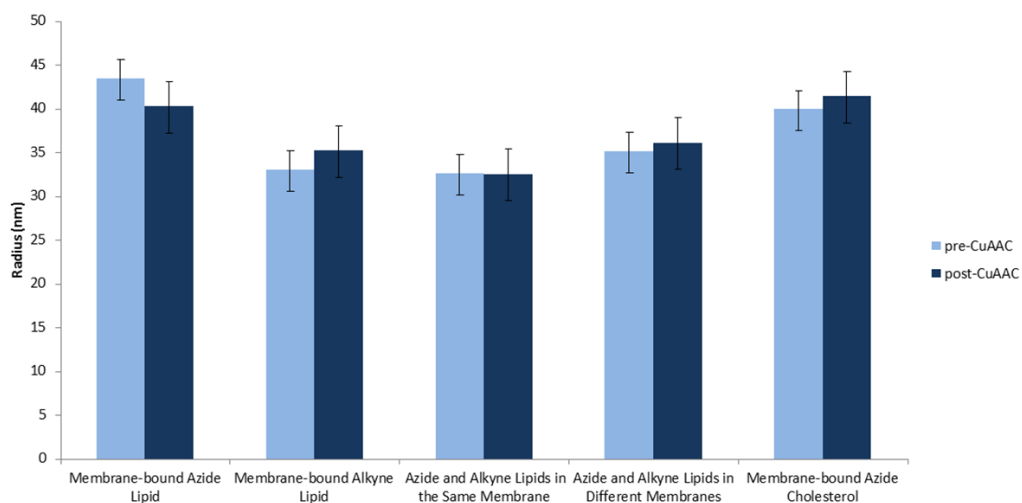


Figure 3.4: Vesicle Size Pre- and Post-CuAAC

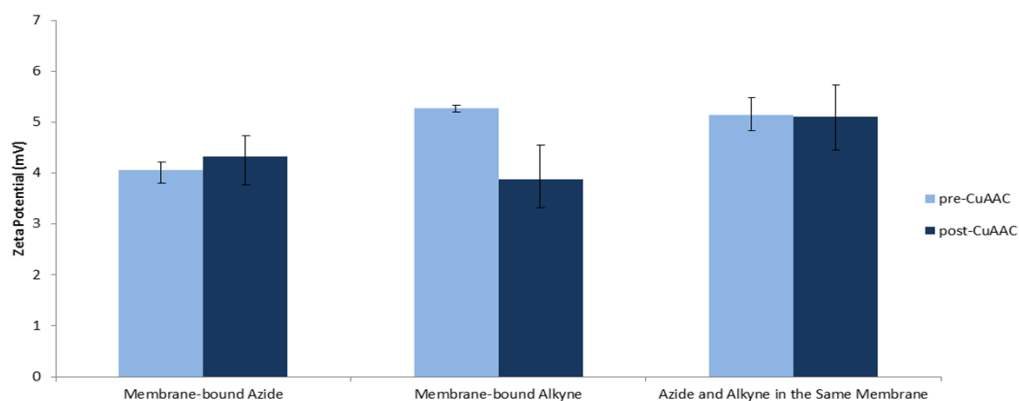


Figure 3.5: Zeta Potential Pre- and Post-CuAAC

As expected, the Zeta Potential of the system was not affected by triazole formation, although the slightly positive charge of vesicles could provide positive-positive charge repulsion between vesicle surfaces, which may make lipid transfer more energetically favorable than vesicle aggregation.

Chapter 4

Kinetics with Membrane-Bound Lipid Substrates

Beveridge, J.M., Chenot, H.M., Baksh, M.M., Finn, M.G.

4.1 Kinetics Experimental

A comparison of the CuAAC reaction in lipid membranes vs. in solution can be done informatively by comparing the kinetic rate order in various components.

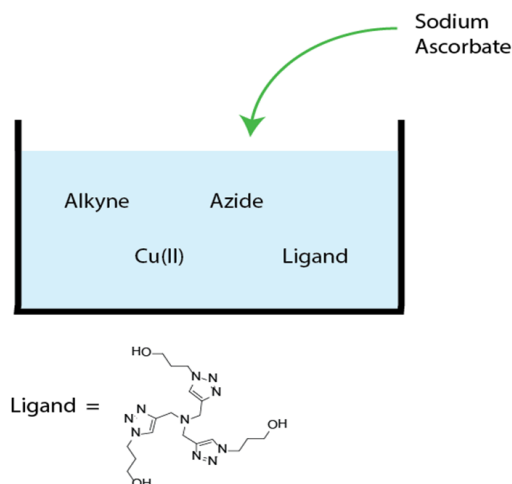


Figure 4.1: Illustration of Kinetics Experimental Setup

Kinetics were carried out for lipid systems in 96-well plates and were initiated by the addition of 40 μL sodium ascorbate (see Figure 4.1) to a 160 μL solution of azide, alkyne, copper(II) sulfate, and THPTA, with the lipid azide and

alkyne components described earlier, or with water-soluble analogues. When one of the reaction substrates was vesicle bound, the highest concentrations used for the membrane-bound component were those described in Table 3.1. Otherwise, the default concentrations in the reaction solution are as follows: 40 μM azidocoumarin, 370 μL 2-methyl-3-butyn-2-ol, 12 μM copper(II) sulfate, and 60 μM THPTA. The amount of the reactive species of interest was then diluted by two, while all other concentrations were held constant, so that kinetics were observed for the half the concentration of the species of interest, and this was repeated for several dilutions for each species of interest. Fluorescence measurements were made by a ThermoFisher Varioscan plate reader. The rate of each CuAAC reaction was monitored via changes in fluorescence intensity ($\lambda_{exc} = 404 \text{ nm}$, $\lambda_{em} = 476 \text{ nm}$) of the coumarin fluorophore.

4.2 Photobleaching and Quenching for Coumarin-Based Systems and other Experimental Incidentals

The lipid-based coumarin has exhibited strong photosensitivity, with a marked difference between samples exposed and unexposed to light, both spectroscopically (Figures 4.2 and 4.3) and visually (Figure 4.4). Due to this noted photosensitivity, all coumarin based-samples were handled under stringent conditions to minimize light exposure.

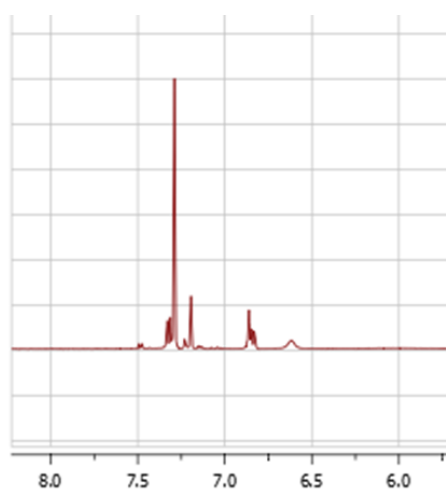


Figure 4.2: NMR Aromatic Region of Active Azidocoumarin-Based Lipid

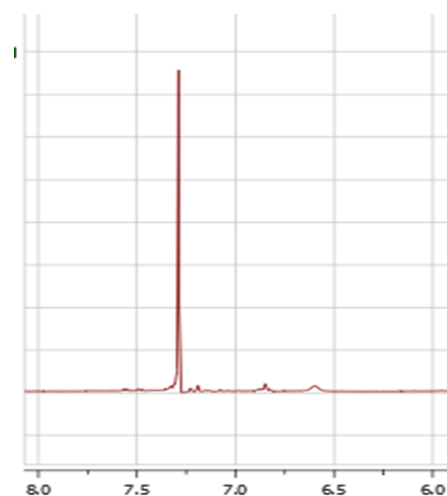


Figure 4.3: NMR Aromatic Region of Photodegraded Azidocoumarin-Based Lipid

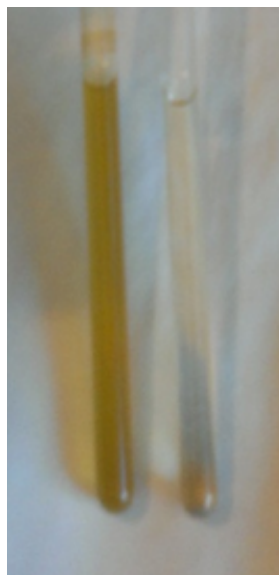


Figure 4.4: Image of Photodegraded (left) and Non-photodegraded (right) Azidocoumarin-Based Lipid in CDCl₃

Upon repeated exposure to excitatory wavelengths, photobleaching was observed. This appeared in kinetic traces as a consistent decrease in fluorescence after the fluorescence maximum was reached. Photobleaching of solutions of the isolated triazole product was observable only at high concentrations. This suggests that photobleaching should be minimal at early stages of the reaction, so its effects were ignored in the determination of kinetic rate constants by pseudo-first order analysis at early time points.

Additionally, for some data points in a few experiments, the plate reader that was used to measure fluorescence reported a value of zero for fluorescence, when even baseline fluorescence for the control was non-zero. When subtracting the baseline, this yielded a negative value for fluorescence, far below even the initial values. These points were summarily discarded as machine error and kinetic analysis was performed with these points removed (Figures 4.5 and 4.6).

4.3 Kinetics in Solution

To validate that this experimental system was comparable to other kinetics methods previously used with CuAAC,¹ kinetics were performed with all components

¹Rodionov, V.O., Fokin, V.V., Finn M.G.. Mechanism of the Ligand-Free Cu(I)-Catalyzed Azide-Alkyne Cycloaddition Reaction. *Angew. Chem. Int. Ed.* 44, 2210-2215, doi: 10.1002/anie.200461496

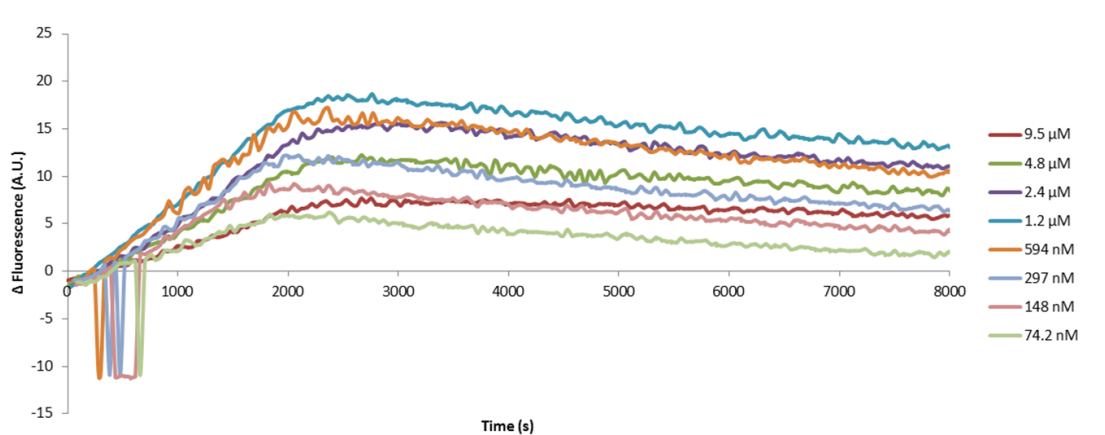


Figure 4.5: Kinetic traces for lipid-bound azide substrate undergoing CuAAC. Note the decrease in fluorescence intensity at long times due to photobleaching; the data points showing negative fluorescence are due to a mechanical or software error in the instrument and were ignored to generate Figure 4.6.

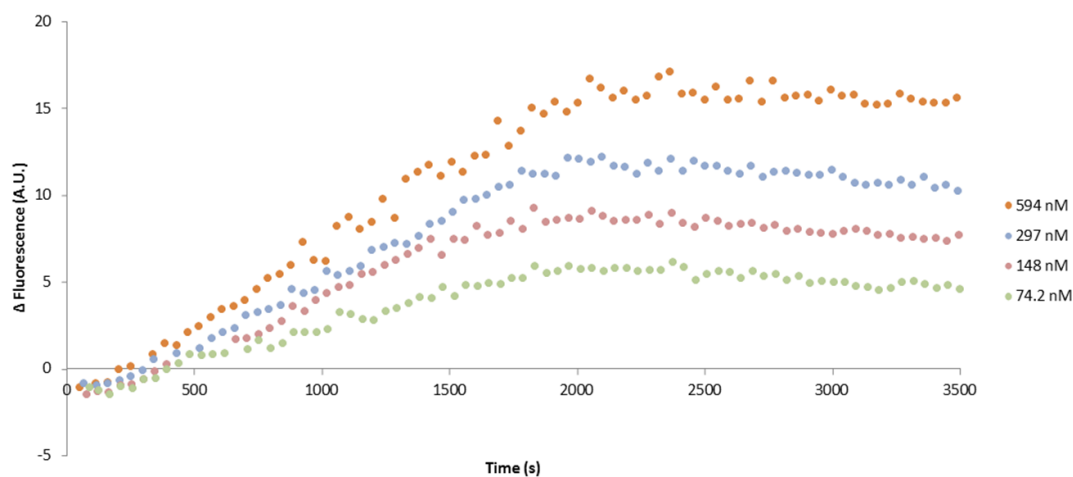


Figure 4.6: Kinetic traces for lipid-bound azide substrate undergoing CuAAC after quenched samples and machine error data points are removed

in solution (azide, alkyne, THPTA, CuSO_4 , and sodium ascorbate). Similar to previous work, rate constants were via initial rate analysis. By plotting the natural log of the initial rate, which was determined to be the portion of the kinetic trace that had a value of no more than 10% of the maximum fluorescence for a sample, against the natural log of the concentration for a series of dilutions, one can obtain the reaction order from the plot's slope.

As expected, and in concurrence with published rate orders for azide and alkyne components in solution,¹ the reaction was approximately first order with respect to (2005).

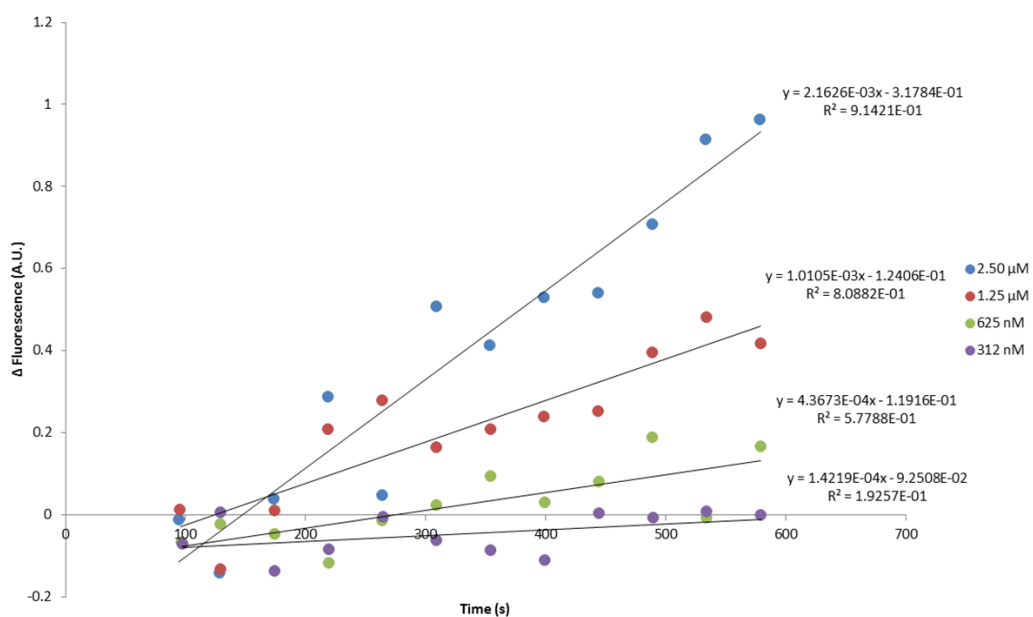


Figure 4.7: Initial Kinetics Plot for 7-hydroxy-3-azidocoumarin in Solution

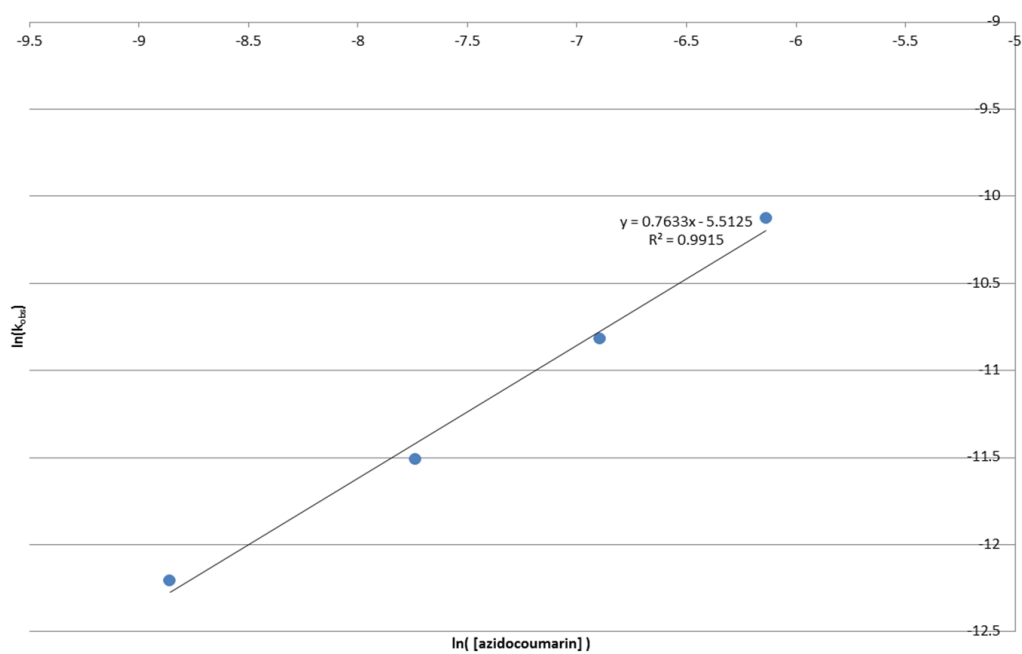


Figure 4.8: Rate Order Plot for 7-hydroxy-3-azidocoumarin in Solution

azide, and between first and second order with respect to alkyne, under catalytic copper conditions (Figures 4.7-4.10).

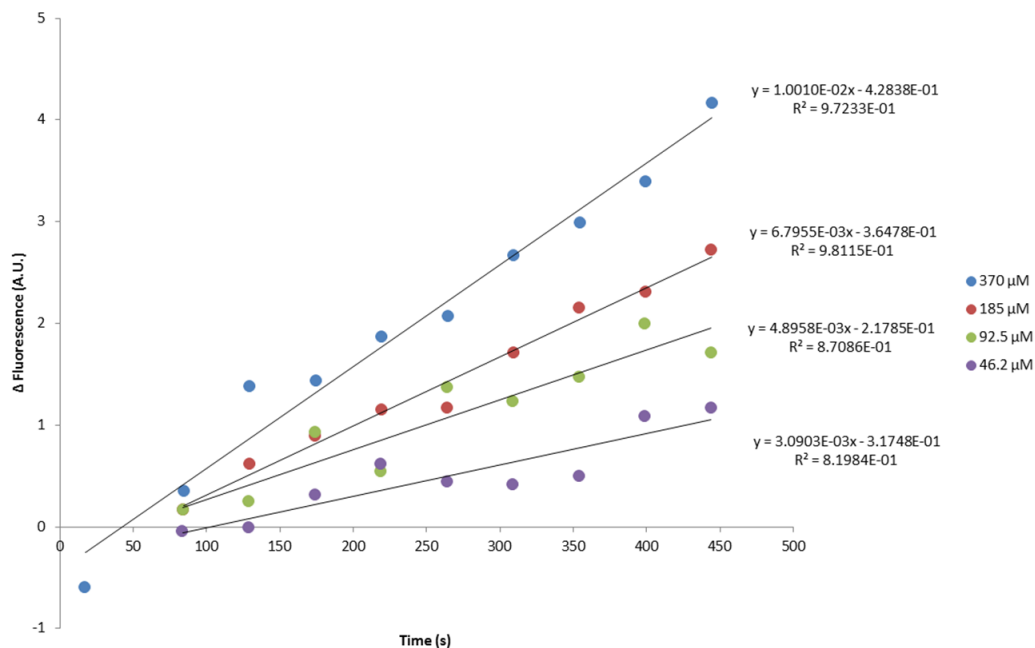


Figure 4.9: Initial Kinetics Plot for 2-methyl-3-butyn-2-ol in Solution

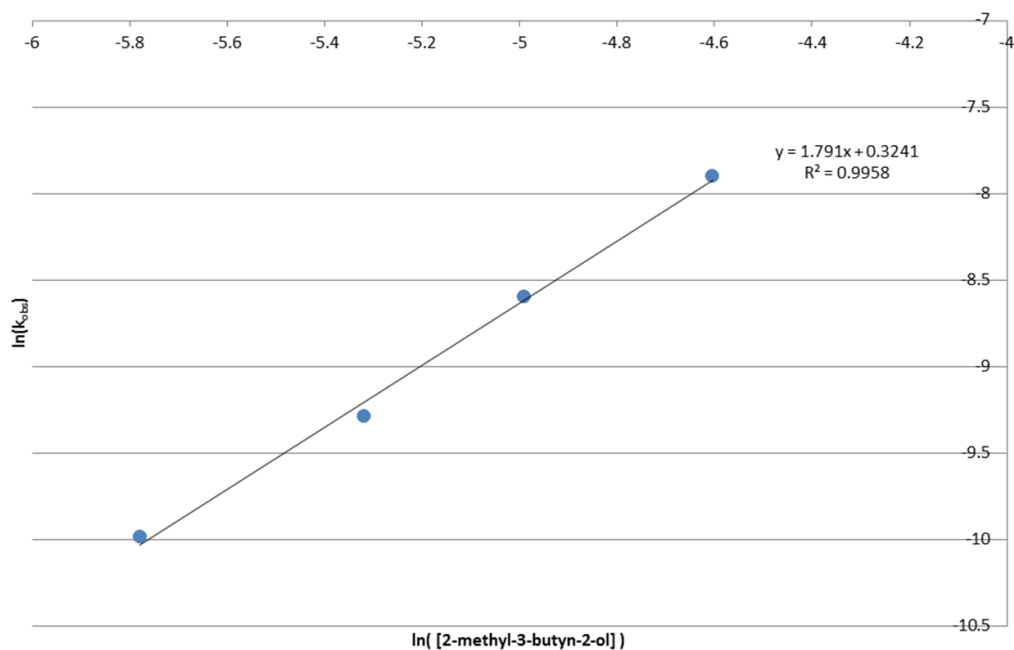


Figure 4.10: Rate Order Plot for 2-methyl-3-butyn-2-ol in Solution

4.4 Kinetics with Membrane Bound-Lipid Substrates

The same kinetic analysis was performed on membrane-bound lipid substrates in SUVs that were prepared as described in the previous chapter.

The kinetic measurements show a fairly reliable determination of approximate

Table 4.1: Reactivity of Azidocoumarin and 2-methyl-3-butyn-2-ol in Solution

	[Azide]	[Alkyne]	[CuSO ₄]	[THPTA]	[Ascorbate]	Rate Order
7-hydroxy-3-azidocoumarin	40 μ L	370 μ L	12 μ L	60 μ L	2.5 mM	0.76 ± 0.1
2-methyl-3-butyn-2-ol	40 μ L	370 μ L	12 μ L	60 μ L	2.5 mM	1.79 ± 0.2

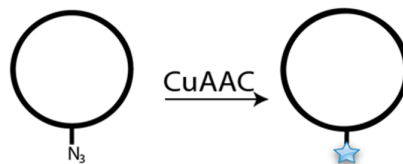


Figure 4.11: CuAAC of Membrane Bound Azidocoumarin with Alkyne in Solution Creates an Increase in Fluorescence

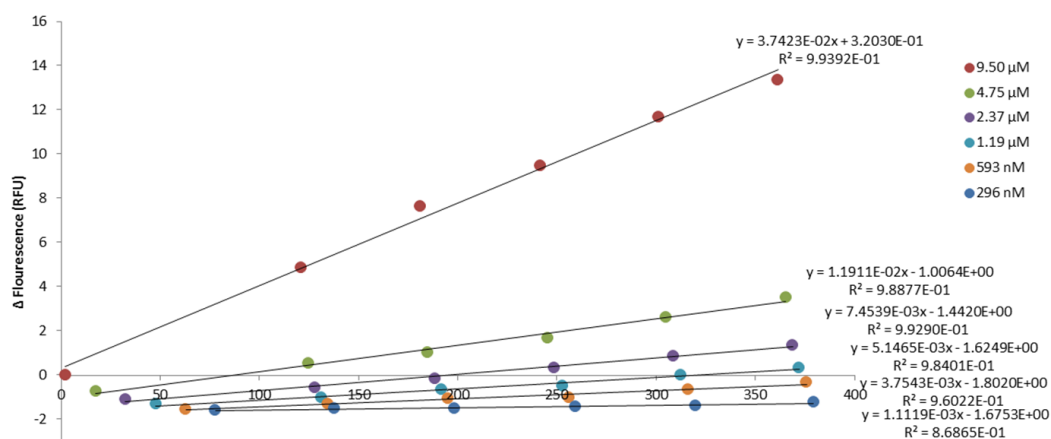


Figure 4.12: Initial Kinetics Plot for Membrane-Bound Azide

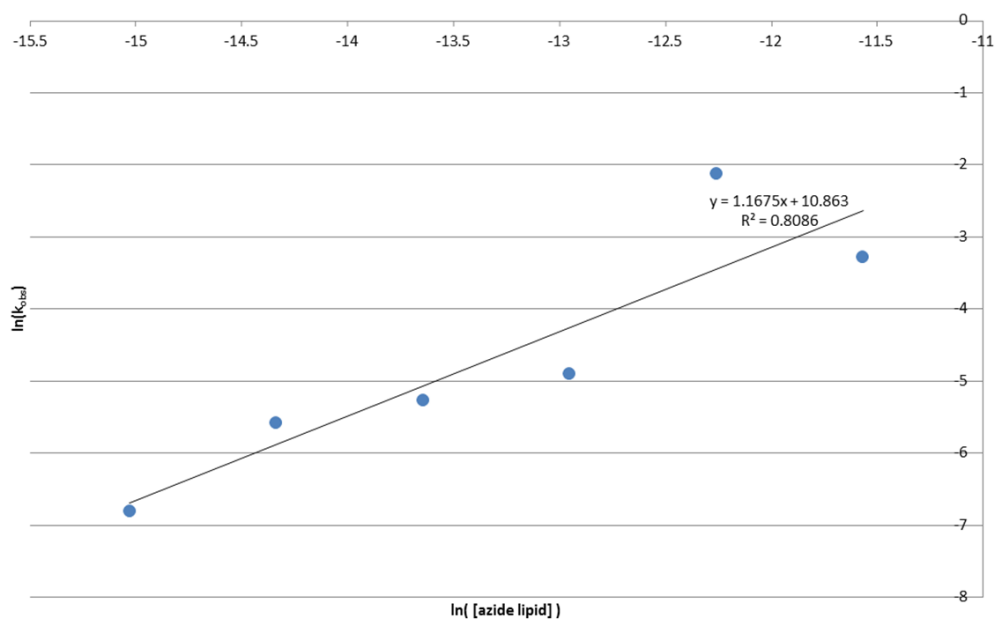


Figure 4.13: Rate Order Plot for Membrane-Bound Azide

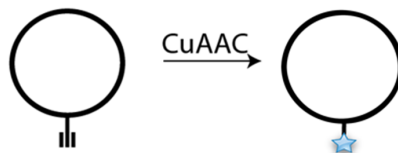


Figure 4.14: CuAAC of Membrane Bound Alkyne with Azidocoumarin in Solution Creates an Increase in Fluorescence

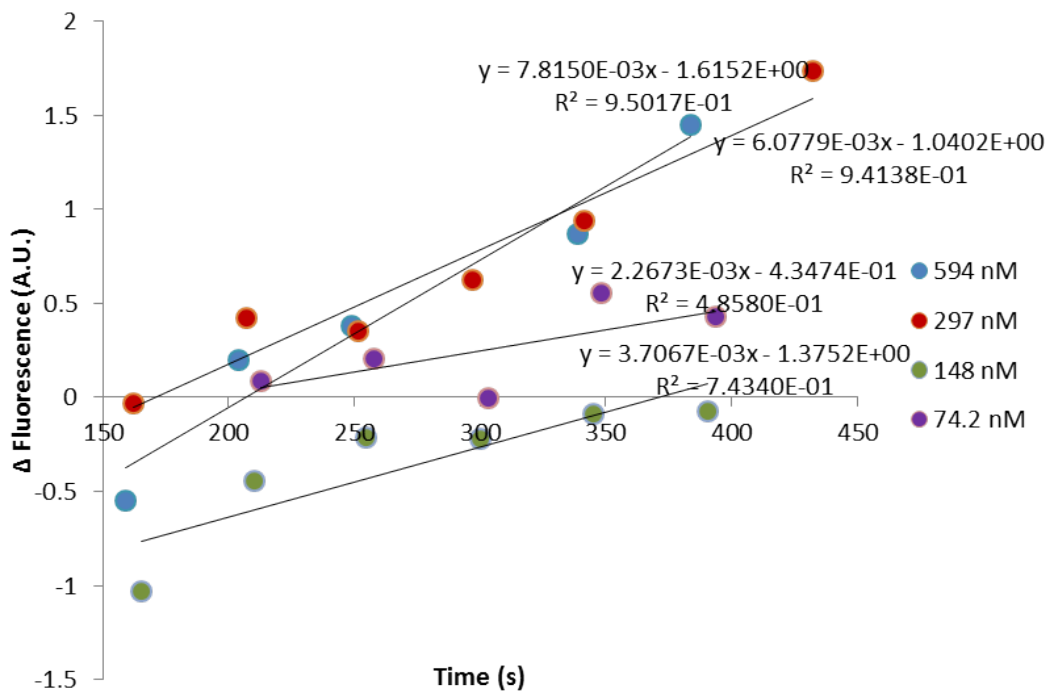


Figure 4.15: Preliminary Initial Kinetics Plot for Membrane-Bound Alkyne

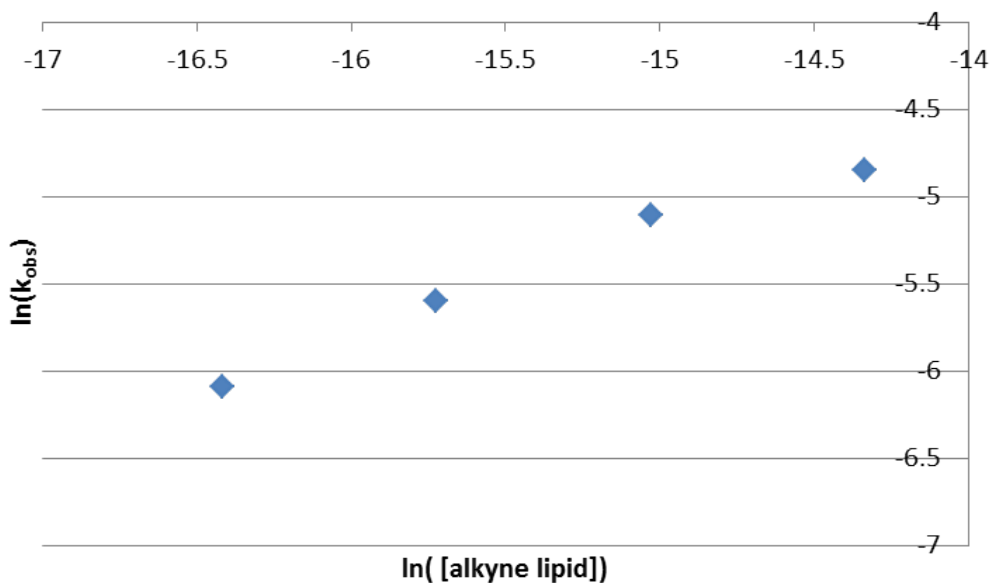


Figure 4.16: Rate Order Plot for Membrane-Bound Alkyne

Table 4.2: Reactivity of Membrane Bound Azide and Alkyne

	[Azide]	[Alkyne]	[CuSO ₄]	[THPTA]	[Ascorbate]	Rate Order
Azide Lipid	9.5 μ L	370 μ L	12 μ L	60 μ L	2.5 mM	1.17 \pm 0.2
Alkyne Lipid	9.5 μ L	594 nM	12 μ L	60 μ L	2.5 mM	inconclusive

first-order dependence on membrane-bound azide in the CuAAC reaction (Figures 4.11-4.13); however, the data for membrane-bound alkyne is less clear. Additional measurements will have to be done to confirm the preliminary results in Figures 4.15 and 4.16, but it appears that nonlinear “threshold” behavior may dominate in this case. In other words, the reaction rate at the lowest concentration was very low, whereas the reaction at the highest concentrations appeared to be relatively insensitive to lipid-alkyne concentration (Figures 4.14-4.16). This is consistent with previous conclusions (for reactions in solution) that two Cu centers need to be brought together to mediate effective catalysis, that the alkyne unit is important in this self-assembly, and that higher-order aggregates can be inhibitory.²

4.5 Intra-vesicular Reactivity vs. Inter-vesicular Reactivity

The reactivity of two lipid-bound substrates was evaluated while both lipids were doped into the same vesicle and while the azide lipid was in one vesicle and the alkyne lipid was in a second vesicle (Figure 4.17).

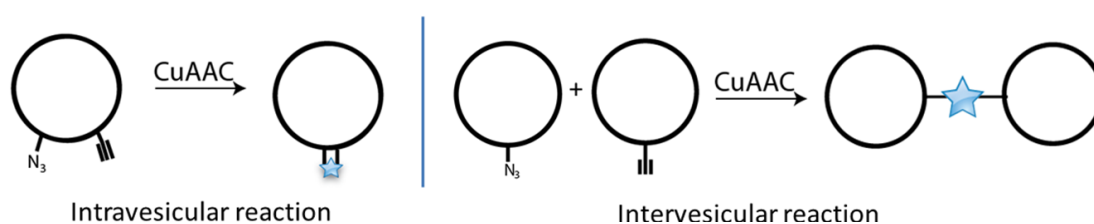


Figure 4.17: Intravesicular vs. Intervesicular Reactivity

In a fluid lipid system, Menger found that intravesicular reactivity occurred more rapidly than intervesicular reactivity for a nucleophile-electrophile reaction.³

²Worrell, B.T., Malik, J.A., Fokin, V.V. Direct Evidence of a Dinuclear Copper Intermediate in Cu(I)-Catalyzed Azide-Alkyne Cycloadditions. *Science*, 340, 6131, 457-460, doi: 10.1126/science.1229506 (2013).

³Menger, F.M., Azov, V.A. Cytomimetic Modeling in Which One Phospholipid Liposome Chemically Attacks Another. *J. Am. Chem. Soc.* 122, 6492-6493, doi: 10.1021/ja000504x (2000).

Table 4.3: Intra-vesicular vs. Inter-vesicular Reactivity

Type of vesicle	[Azide Lipid]	[Alkyne Lipid]	[CuSO ₄]	[THPTA]	[Ascorbate]	Initial rate ($\Delta A.U.\text{sec}^{-1}$)
Intra-vesicular	9.5 μL	9.5 μL	12 μL	60 μL	2.5 mM	3.8×10^{-4}
Inter-vesicular	9.5 μL	9.5 μL	12 μL	60 μL	2.3 mM	9.3×10^{-4}

For a non-fluid lipid system, where lipids are in gel-phase and not able to translocate within a leaflet as in fluid lipids, the opposite was observed. The rate of reaction was faster for systems where azide lipid substrates were in one vesicle and alkyne lipid substrates were in another vesicle than for systems where both azide and alkyne lipid substrates were in the same vesicle.

For a system where both azide and alkyne lipid substrates were in the same membrane, one would expect that dominant intravesicular would lead the reaction rate to be independent of the total vesicle concentration, so long as the concentration of azide and alkyne within the vesicle remained constant.

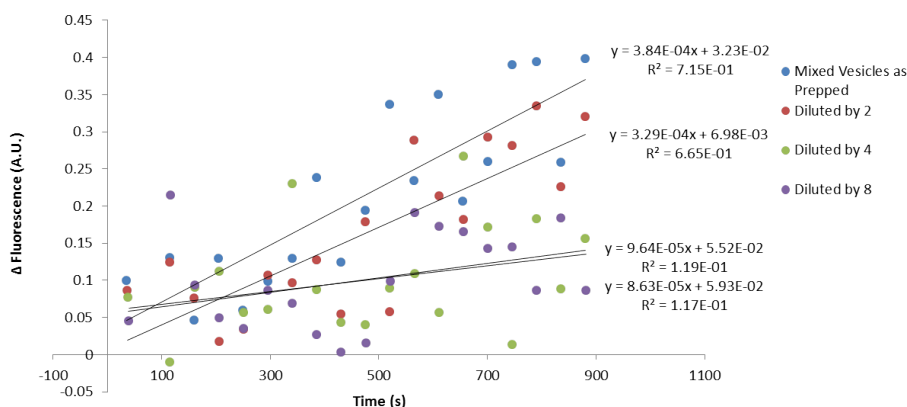


Figure 4.18: Initial Rate of Reaction for Azide and Alkyne Lipids in the Same Vesicle is Concentration Dependent, Suggesting an Inter-vesicular Reaction

Preliminary data (Figure 4.18, Table 4.3) suggest that the opposite trend might be observed. The data is widely scattered, requiring repetition of the experiment to make sure, but it appears that the reaction rate is dependent on vesicle concentration while the ratio of azide to alkyne within the vesicles was held constant. This suggests that inter-vesicular reactions may play a significant role.

To probe this question, vesicles were constructed bearing only azide, only alkyne, or an equimolar mixture of the two, where the overall functional group concentration was 1% of the total lipid. If intra-vesicle reactivity were dominant, the “mixed” vesicles should undergo CuAAC reaction much faster than a mixture

of the “pure” vesicles. The opposite was observed. Inter-vesicle reactivity is consistent with this trend, since one may expect a higher probability of productive azide-alkyne interaction upon the collision of the pure vesicles, as illustrated in Figure 4.19, at least in the early stages of the reaction that were followed.

Inter-vesicle CuAAC reactions would be expected to lead to vesicle aggregation and a sharp increase in the observed size of vesicles as the reaction occurs; however, as noted in Figure 3.4, no significant change in size was observed before and after the reaction. This suggests that the azide- or alkyne-bearing lipid is transferred from one vesicle to another. Two general pathways can be envisioned for this (Figure 4.20), involving lipid transfer before or after CuAAC reaction. Since vesicles incorporating both azide and alkyne were observed to undergo slow reaction, we propose that lipid transfer occurs rapidly after triazole formation.

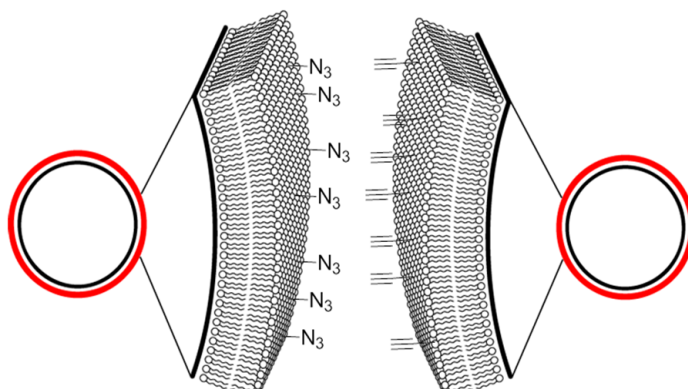


Figure 4.19: Reactive Species in Separate Vesicles Have a Higher Probability of Finding an Adequate Partner Rapidly

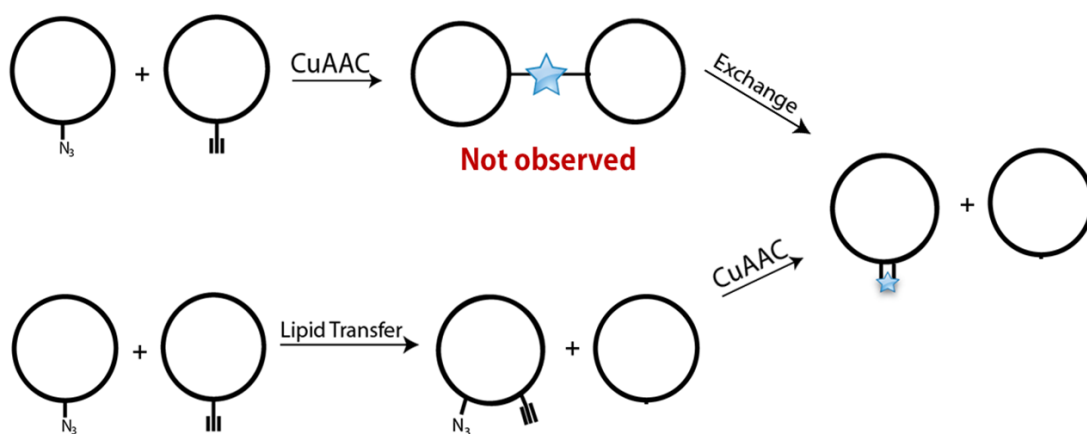


Figure 4.20: Possible routes for the observed reaction of azide-vesicles with alkyne-vesicles to produce triazoles without vesicle aggregation.

Chapter 5

Conclusions and Future Work

Beveridge, J.M., Baksh, M.M., Chenot, H.M., Finn, M.G.

5.1 In Summary

Azide- and alkyne-functionalized lysolipids were synthesized and incorporated into SUVs with no more than 1% synthesized lipid and 99% DPPC. These lipids, in vesicles, were then subject to CuAAC to observe the kinetics in two-dimensions for possible mechanistic differences from the three-dimensional CuAAC reaction and to study the effects of triazole formation on membrane properties, including vesicle size and charge.

Experimental results demonstrate that, as expected, triazole formation has no significant effect on membrane charge. CuAAC between two vesicles also yielded no significant change in vesicle size, which is suggestive of lipid transfer between non-fluid lipid vesicles, a phenomenon which has not previously been reported.

Kinetic analysis suggests that for these non-fluid lipid vesicles containing both azide and alkyne lipid substrates, intravesicular reactivity is effectively diminished. The concentration dependence of the observed reaction rates suggests that the observed reactivity derives solely from interactions between two separate vesicles. These findings with non-fluid lipid systems are in contrast to the previously observed findings with membrane-bound substrates in fluid vesicles, which found far greater reactivity for intra-vesicular reactions than for inter-vesicular reac-

tions.¹ One explanation for this could be that the intra-vesicular reaction does not allow the proper geometry for the formation of the requisite binuclear-copper complex for CuAAC. A simpler alternative may rely on the static nature of lipids within these membranes. The lack of membrane fluidity could restrict the mobility of embedded azide and alkyne species, so the reaction could not transpire unless they are located within close enough proximity, which is statistically unlikely. The reaction of two different vesicles, however, would allow azide and alkyne to react.

5.2 Looking Forward

I have so far evaluated the effect of triazole formation on membrane properties has only been evaluated thus far for vesicle size and charge. An exploration of triazole formation on other membrane properties will soon be underway. Properties to be evaluated include permeability and fluidity, which will be studied via ratiometric calcium assays with cell-impermeant Fluo-4 dye² and fluorescent recovery after photobleaching (FRAP), respectively. One set of experiments that will be particularly exciting involves the addition of small amounts of fluid lipids to the non-fluid lipid bilayers for mixed azide- and alkyne-modified vesicles. By doping in the fluid lipids, it is hoped that the membrane will achieve some degree of fluidity and that there will be an observable transition between a preference for intervesicular reactivity as demonstrated in this thesis, to the preference for intravesicular reactivity as described in the literature. Evaluating reactivity at these interfaces between lipid fluid and gel phases is particularly relevant because biological membrane microdomains exhibit similar interfaces and are areas of vital reactivity for the cell with respect to signalling.^{3,4}

¹Menger, F.M., Azov, V.A. Cytomimetic Modeling in Which One Phospholipid Liposome Chemically Attacks Another. *J. Am. Chem. Soc.* 122, 6492-6493, doi: 10.1021/ja000504x (2000).

²Juffermans, L.J.M., Dijkmans, P.A., Musters, R.J.P., Visser, C.A., and Kamp, O. Transient Permeabilization of Cell Membranes by Ultrasound-Exposed Microbubbles is Related to Formation of Hydrogen Peroxide. *Am. J. Physiol. Heart Circ. Physiol.* 291, H1595-H1601, doi: 10.1152/ajpheart.01120.2005 (2005).

³Russell, S., Oliero, J. Compartmentalization in T-Cell Signalling: Membrane Microdomains and Polarity Orchestrate Signalling and Morphology. *Immunol. Cell Biol.* 84, 107-113, doi: 10.1111/j.1440-1711.2005.01415.x (2006).

⁴Heneberg, P., Lebduska, P., Draberova, L., Korb, J., Draber, P. Topography of Plasma Membrane Microdomains and Its Consequences for Mast Cell Signalling. *Eur. J. Immunol.* 36, 10, 2795-2806, doi: 10.1002/eji.200636159 (2006).

Copper(I)-binding ligands serve many purposes in CuAAC reactions. They are able to bind copper(I) and present it to reaction substrates, they are able to help preserve copper(I) from oxidation or reduction, which would make it no longer active for CuAAC, and it plays a role in accelerating the reaction.⁵ Copper(I)-binding ligands are also able to limit the cytotoxicity of copper(I) species, which makes it relevant for in vivo CuAAC.⁶ Some work has been made toward creating a lipid analogue of an already existing copper(I) binding ligand. This material has been synthesized and used as a crude material in a membrane system with some success by assuming that membrane self-purifies, but has not been used in its pure form. This will be purified in the future and incorporated into lipid vesicles for lipid-phase CuAAC catalysis, in the same vesicle as the azide and alkyne substrate, as well as in separate vesicles. Preliminary experiments with the crude lipid analogue of the copper(I)-binding ligand observed reactivity, as measured by a change in fluorescence, when the lipid analogue was in one vesicle and azide and alkyne were in another vesicle.

Biological membranes are comprised of more than just lipids; cholesterol, proteins, and glycosylated lipids and proteins each play roles in how cells interact with each other and their environment.⁷ Cholesterol also plays a large role in the dynamics of lipid microdomains.⁸ To this end, azide- and alkyne- functionalized cholesterol derivatives are of interest, to see how triazole formation between cholesterol derivatives, or between a lipid and cholesterol molecule will affect membrane properties. These studies will provide insight into cellular membrane communication and reactivity, as well as into membrane microdomain behavior and behavior at the interface of gel- and liquid-phases.

⁵Rodionov, V.O., Presolski, S.I., Gardinier, S., Lim, Y.H., Finn, M.G. Benzimidazole and Related Ligands for Cu-Catalyzed Azide-Alkyne Cycloaddition. *J. Am. Chem. Soc.*, 129, 12696-12704, doi: 10.1021/ja072678l (2007).

⁶Hong, V., Steinmetz, N.F., Manchester, M., Finn, M.G. Labeling Live Cells by Copper-Catalyzed Alkyne-Azide Click Chemistry. *Bioconjug. Chem.* 21, 10, 1912-1916, doi: 10.1021/jb100272z (2010).

⁷Alberts, B., Johnson, A., Lewis, J., Raff, M., Roberts, K., Walter, P. *Molecular Biology of the Cell*, 5th Ed., Garland Science: New York (2007).

⁸Riff, J.D., Callahan, J.W., Sherman, P.M. Cholesterol-Enriched Membrane Microdomains Are Required for Inducing Host Cell Cytoskeleton Rearrangements in Response to Attaching-Effacing *Escherichia coli*. *Infect Immun.* 73, 11, 7113-7125, doi: 10.1128/IAI.73.11.7113-7125.2005 (2005).

Appendix A

Plate Reader Fluorescence Data

The following is the raw fluorescence data, obtained by fluorescence measurements with a ThermoFisher Varioskan Plate Reader.

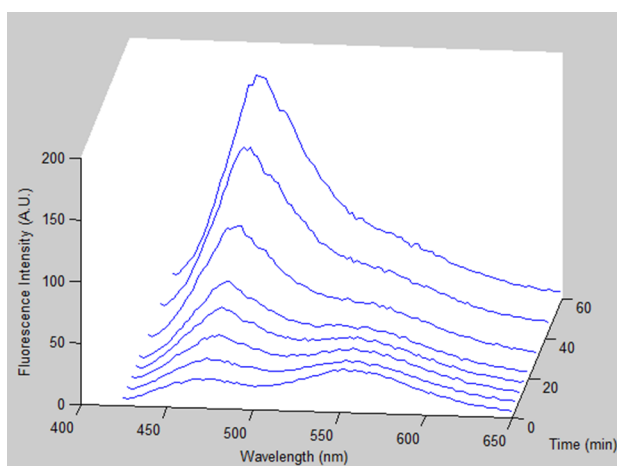


Figure A.1: Fluorescence evolution for coumarin substrates undergoing CuAAC.

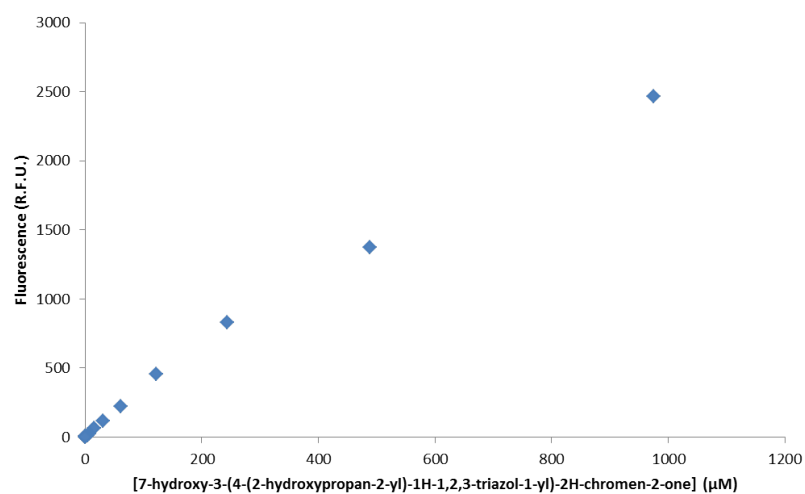


Figure A.2: Fluorescence As A Function of Concentration of Coumarin-Triazole

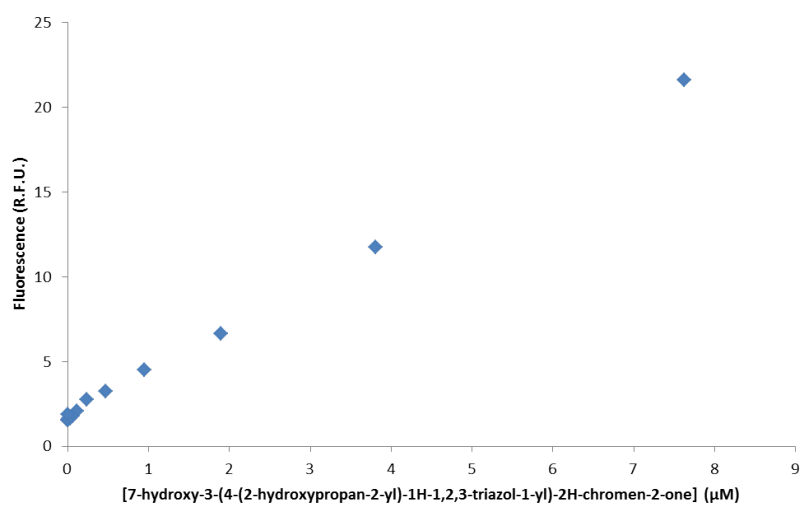


Figure A.3: Fluorescence As A Function of Concentration of Coumarin-Triazole (Zoomed to lower concentrations)

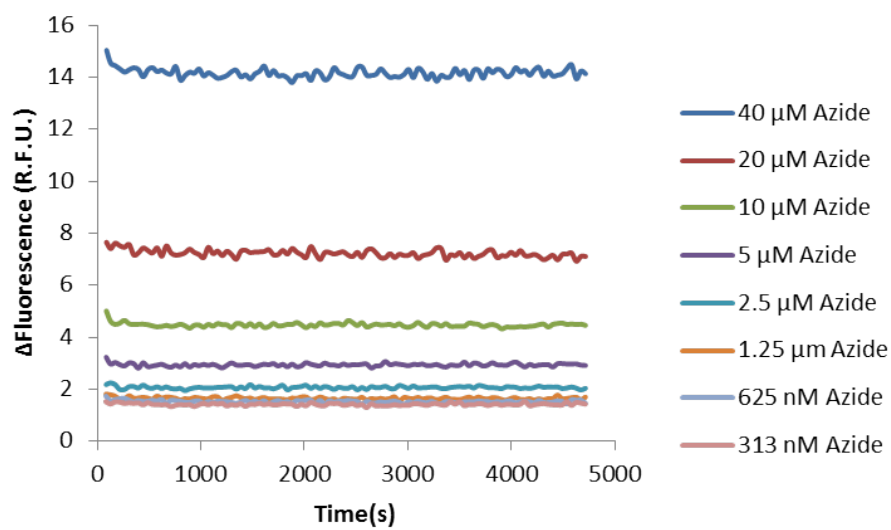


Figure A.4: Background Fluorescence Traces for Reactions in Solution (Azide). Raw data for Figure 4.7.

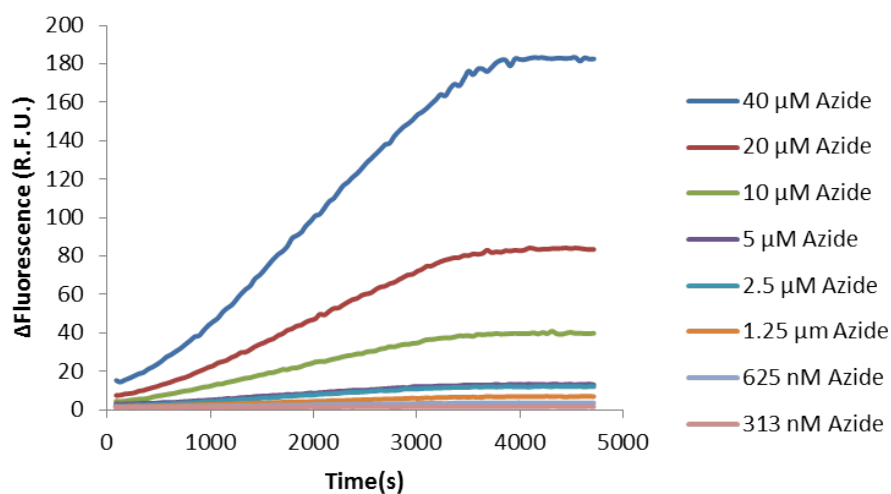


Figure A.5: Raw Fluorescence Traces for Reactions in Solution (Azide) Raw data for Figure 4.7.

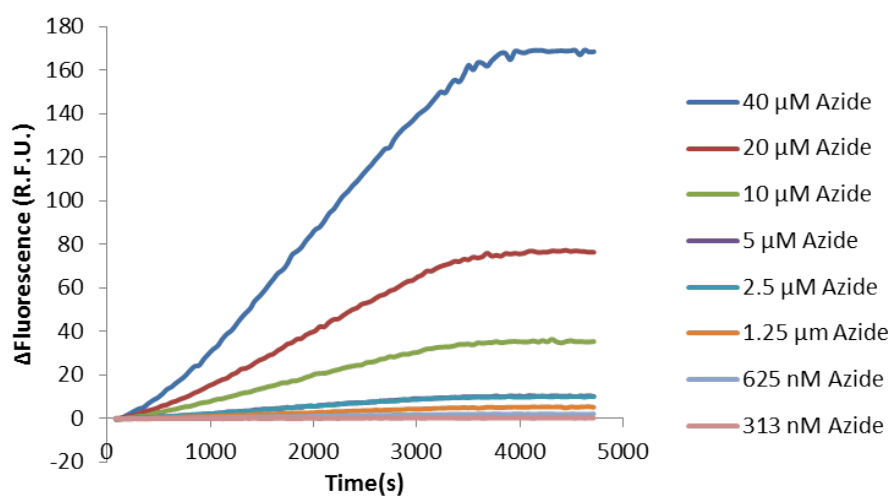


Figure A.6: Fluorescence Traces for Reactions in Solution (Azide) with Backgrounds Subtracted. Corresponds to Figure 4.7.

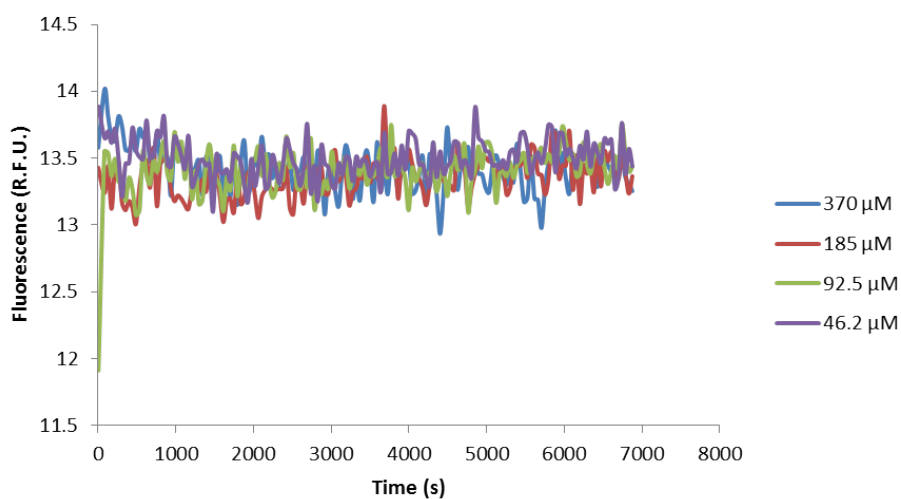


Figure A.7: Background Fluorescence Traces for Reactions in Solution (Alkyne). Raw data for Figure 4.9.

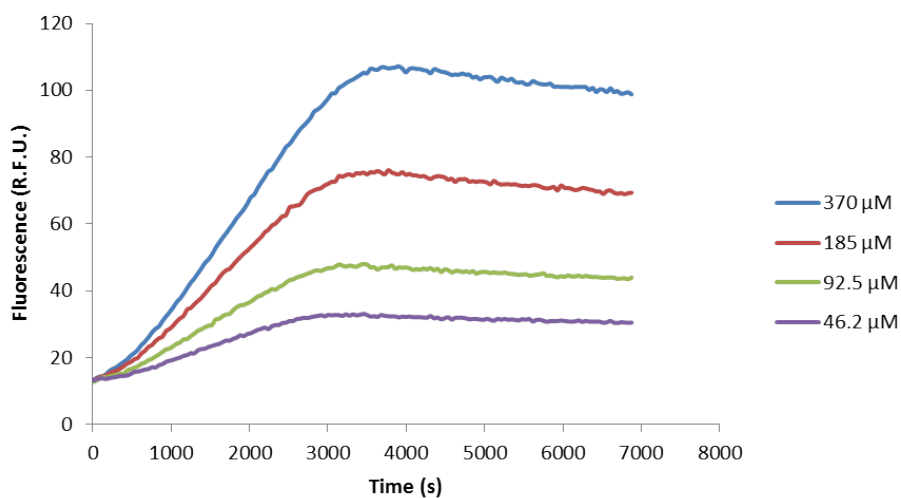


Figure A.8: Raw Fluorescence Traces for Reactions in Solution (Alkyne) Raw data for Figure 4.9.

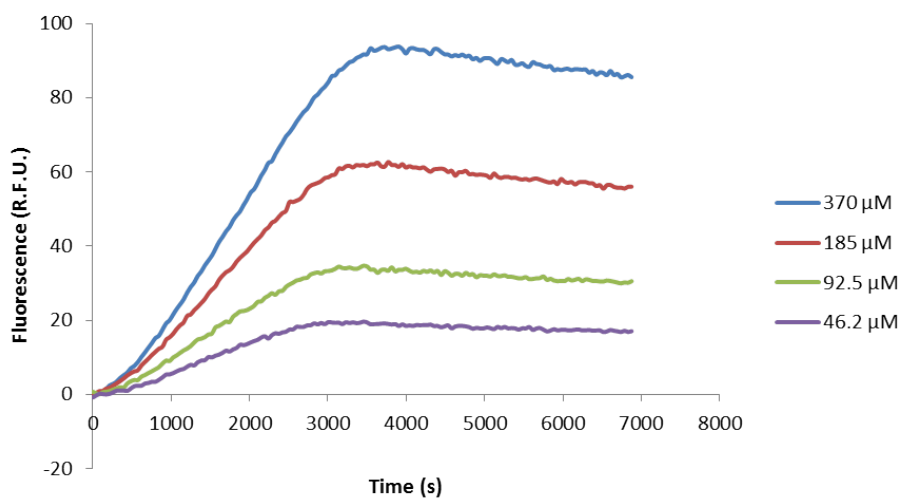


Figure A.9: Fluorescence Traces for Reactions in Solution (Alkyne) with Backgrounds Subtracted. Corresponds to Figure 4.9.

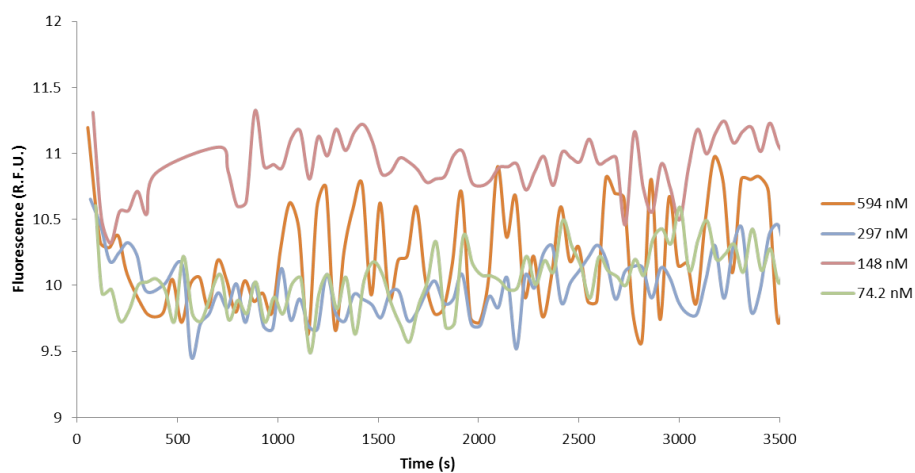


Figure A.10: Background Fluorescence Traces for Reaction with Membrane-Bound Azide. Raw data for Figure 4.12.

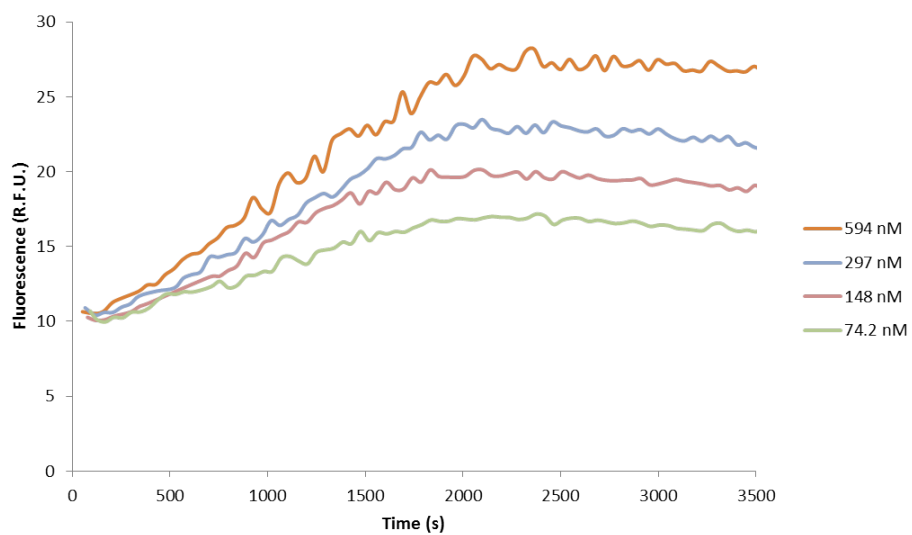


Figure A.11: Raw Fluorescence Traces for Reactions with Membrane-Bound Azide. Raw data for Figure 4.12.

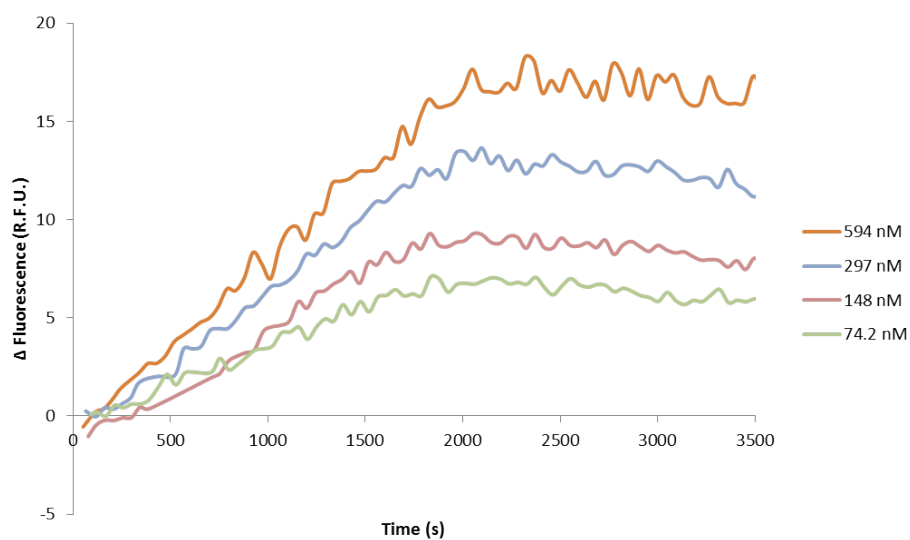


Figure A.12: Fluorescence Traces for Reactions with Membrane-Bound Azide with Background Subtracted. Corresponds to Figure 4.12.

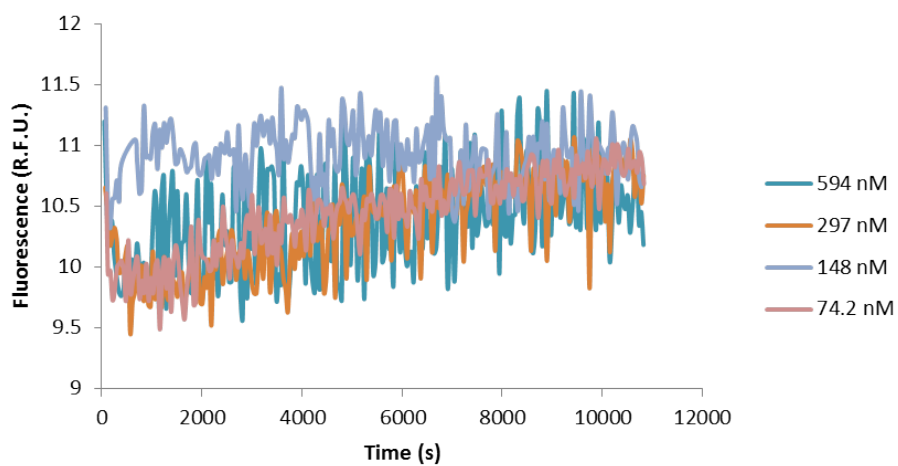


Figure A.13: Background Fluorescence Traces for Reaction with Membrane-Bound Alkyne). Raw data for Figure 4.15.

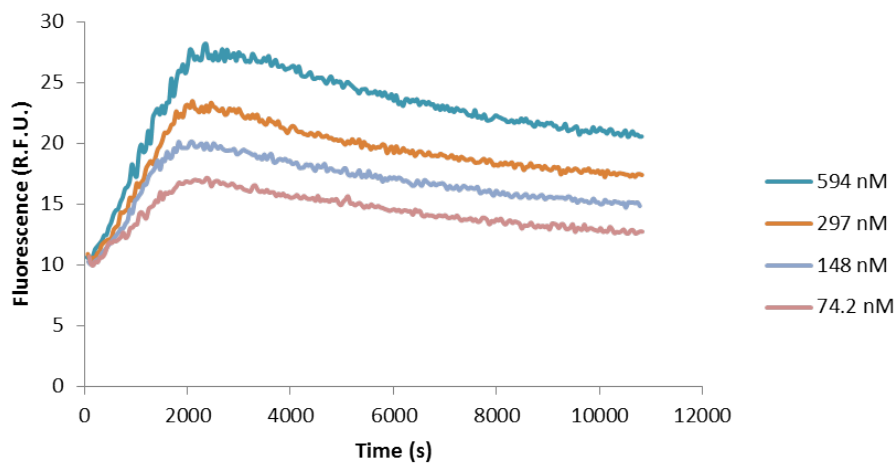


Figure A.14: Raw Fluorescence Traces for Reactions with Membrane-Bound Alkyne. Raw data for Figure 4.15.

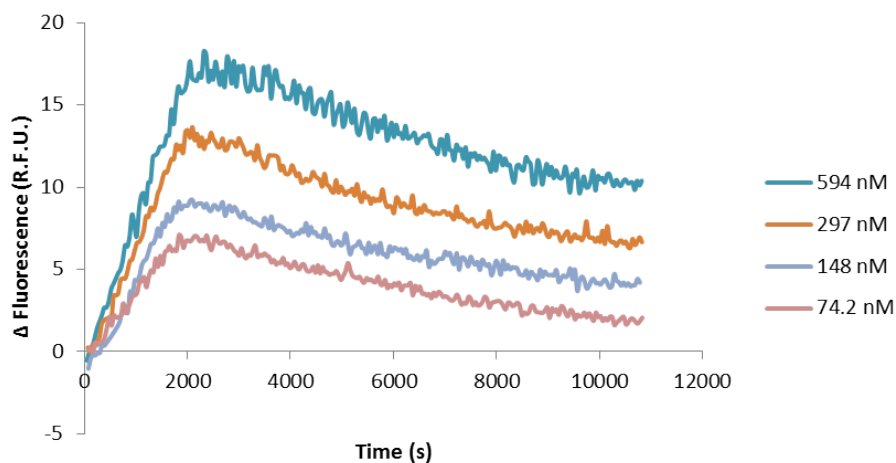


Figure A.15: Fluorescence Traces for Reactions with Membrane-Bound Alkyne with Backgrounds Subtracted. Corresponds to Figure 4.15.

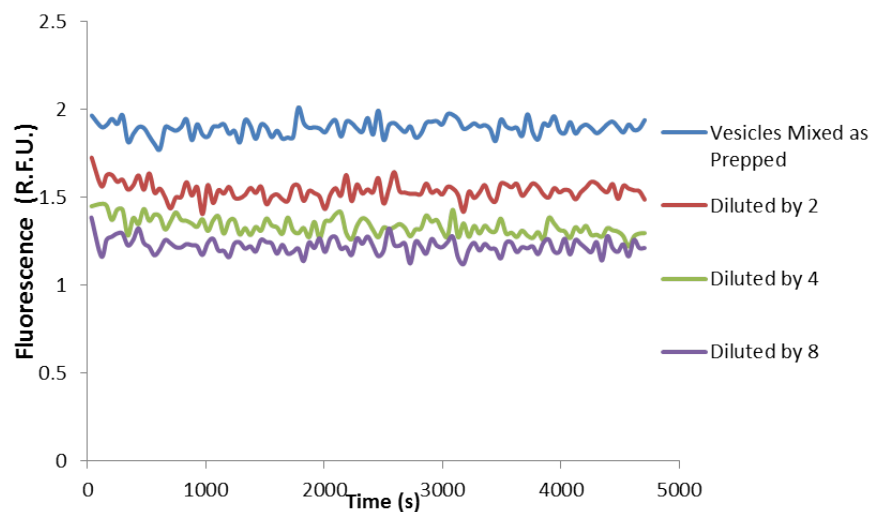


Figure A.16: Background Fluorescence Traces for "Intravesicular" Reaction. Raw Data for Figure 4.18 and Table 4.3.

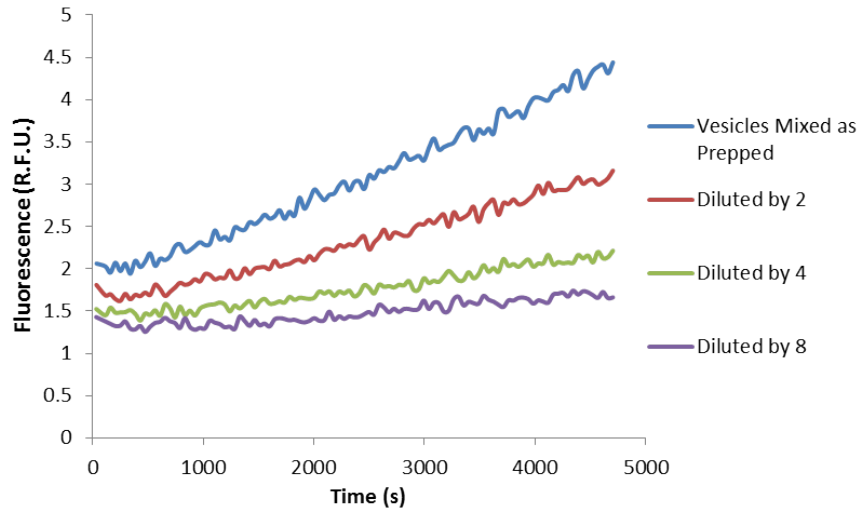


Figure A.17: Raw Fluorescence Traces for "Intravesicular" Reaction. Raw Data for Figure 4.18 and Table 4.3.

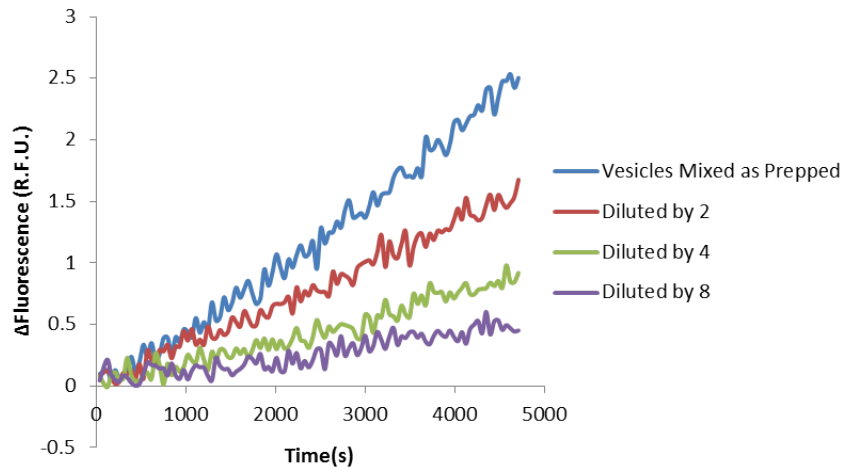


Figure A.18: Fluorescence Traces for "Intravesicular" Reaction with Backgrounds Subtracted. Corresponds to Figure 4.18 and Table 4.3.

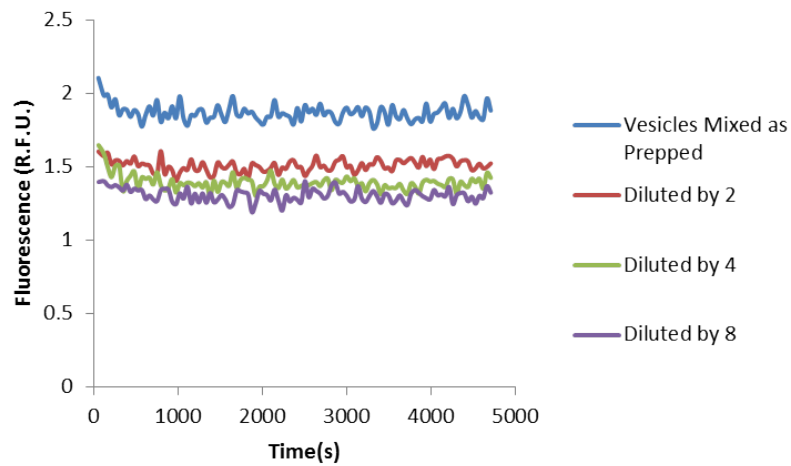


Figure A.19: Background Fluorescence Traces for Interventricular Reaction. Raw Data for Table 4.3.

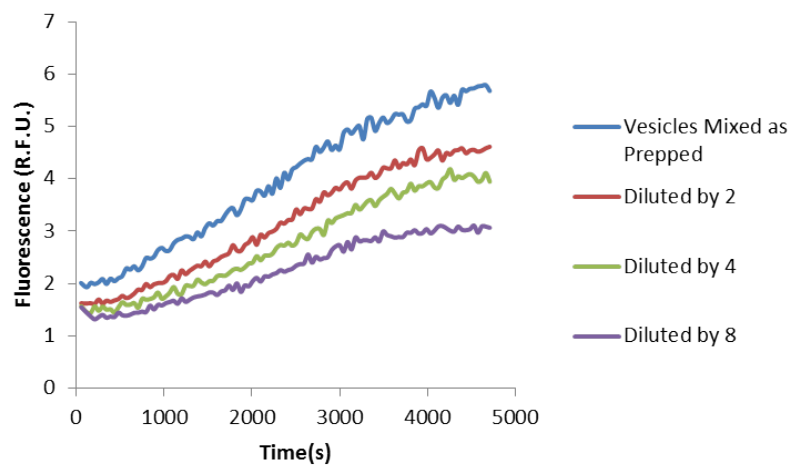


Figure A.20: Raw Fluorescence Traces for Interventricular Reaction. Raw Data for Table 4.3.

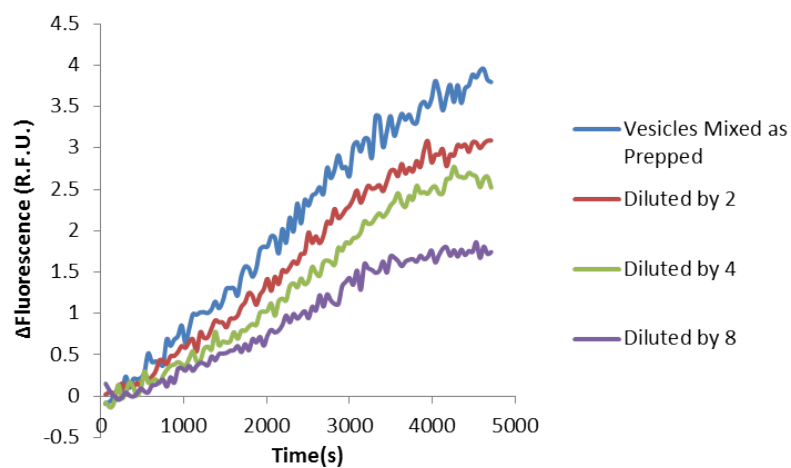


Figure A.21: Fluorescence Traces for Intraventricular Reaction with Backgrounds Subtracted. Corresponds to Table 4.3.

References

- Abramson, M. B., Katzman, R. & Gregor, H. P. Aqueous Dispersions of Phosphatidylserine: Ionic Properties. *J. Biol. Chem.* 239, 70-76 (1964).
- Alberts, B., Johnson, A., Lewis, J., Raff, M., Roberts, K., Walter, P. *Molecular Biology of the Cell*, 5th Ed., Garland Science: New York (2007).
- Di Paolo, G., Moskowitz, H.S., Gipson, K., Wenk, M.R., Voronov, S., Obayashi, M., Ravell, R., Fitzsimonds, R.M., Ryan, T.A., De Camilli, P. Impaired PtdIns(4,5)P₂ Synthesis In Nerve Terminals Produces Defects in Synaptic Vesicle Trafficking. *Nature* 431, 415-422, doi: 10.1038/nature02896 (2004).
- Eggeling, C., et al. Direct Observation of the Nanoscale Dynamics of Membrane Lipids in a Living Cell. *Nature* 457, 1159-1162, doi: 10.1038/nature07596 (2009).
- Fessler, M.B., Parks, J.S. Intracellular Lipid Flux and membrane Microdomains as Organizing Principles in Inflammatory Cell Signalling. *J. Immunol.* 187, 1529-1535, doi: 10.4049/jimmunol.1100253 (2011).
- Gaebler, A. *et al.* Alkyne Lipids as Substrates for Click Chemistry-Based in vitro Enzymatic Assays. *J Lipid Res.* 54, 8, 2282-2290, doi: 10.1194/jlr.D038653 (2013).
- Gubbens, J. *et al.* Photocrosslinking and Click Chemistry Enable the Specific Detection of Proteins Interacting with Phospholipids at the Membrane Interface. *Chemistry & Biology* 16, 3-14, doi: 10.1016/j.chembiol.2008.11.009 (2009).
- Haluska, C.K., Baptista, M.S., Fernandes, A.U., Schroder, A.P., Marques, C.M., Itri, R. Photo-activated Phase Separation in Giant Vesicles Made from Different Lipid Mixtures. *Biochim. Biophys. Acta* 1818, 3, 666-672, doi: 10.1016/j.bbamem.2011.11.025 (2011).
- Heneberg, P., Lebduska, P., Draberova, L., Korb, J., Draber, P. Topography of Plasma Membrane Microdomains and Its Consequences for Mast Cell Signalling. *Eur. J. Immunol.* 36, 10, 2795-2806, doi: 10.1002/eji.200636159 (2006).
- Hodge, P. Polymer-supported Organic Reactions: What Takes Place in the Beads? *Chem. Soc. Rev.* 26, 417-424, doi: 10.1039/CS9972600417 (1997).

- Hong, V., Steinmetz, N.F., Manchester, M., Finn, M.G. Labeling Live Cells by Copper-Catalyzed Alkyne-Azide Click Chemistry. *Bioconjug. Chem.* 21, 10, 1912-1916, doi: 10.1021/jb100272z (2010).
- Johnsson, M., Edwards, K. Liposomes, Disks, and Spherical Micelles: Aggregate Structure in Mixtures of Gel Phase Phosphatidylcholines and Poly(Ethylene Glycol)-Phospholipids. *Biophys. J.* 85, 6, 3839-3847, doi: 10.1016/S0006-3495(03)74798-5 (2003).
- Juffermans, L.J.M., Dijkmans, P.A., Musters, R.J.P., Visser, C.A., and Kamp, O. Transient Permeabilization of Cell Membranes by Ultrasound-Exposed Microbubbles is Related to Formation of Hydrogen Peroxide. *Am. J. Physiol. Heart Circ. Physiol.* 291, H1595-H1601, doi: 10.1152/ajpheart.01120.2005 (2005).
- Kolb, H.C., Finn, M.G., Sharpless, K.B. Click Chemistry: Diverse Chemical Function from a Few Good Reactions. *Angew. Chem. Int. Ed.* 40, 11, 2004-2021. doi: 10.1002/1521-3773(20010601)40:11<2004::AID-ANIE2004>3.0.CO;2-5 (2001).
- Lillemeier, B.F., Pfeiffer, J.R., Surviladze, Z., Wilson, B.S., Davis, M.M. Plasma Membrane-Associated Proteins are Clustered into Islands Attached to the Cytoskeleton. *Proc. Nat. Acad. Sci.* 103, 50, 18992-18997, doi: 10.1073/pnas.0609009103 (2006).
- Lindblom, G., Wennerström, H. Amphiphile Diffusion in Model Membrane Systems Studied by Pulsed NMR. *Biophys. Chem.* 6, 2, 167-171 (1977).
- McLean, L.R., Phillips, M.C. Mechanism of Cholesterol and Phosphatidylcholine Exchange or Transfer between Unilamellar Vesicles. *Biochemistry* 20, 10, 2893-2900, doi: 10.1021/bi00513a028 (1981).
- Menger, F.M., Azov, V.A. Cytomimetic Modeling in Which One Phospholipid Liposome Chemically Attacks Another. *J. Am. Chem. Soc.* 122, 6492-6493, doi: 10.1021/ja000504x (2000).
- Menger, F.M., Caran, K.L, Serebyuk, V.A. Chemical Reaction between Colliding Vesicles. *Angew. Chem. Int. Ed.* 40, 20, 3905-3907, doi: 10.1002/1521-3773(20011015)40:20;3905::AID-ANIE3905;3.0.CO;2-B (2001).
- Needham, D., Zhelev, D.V. Lysolipid Exchange with Lipid Vesicle Membranes. *Ann. Biomed. Eng.* 23, 287-298, doi: 10.1007/BF02584429 (1995).
- Neef, A.B., Schultz, C. Selective Fluorescence Labeling of Lipids in Living Cells. *Angew. Chem. Int. Ed.* 48, 1498-1500, doi: 10.1002/anie.200805507 (2009).
- O'Leary, T.J. Lateral Diffusion of Lipids in Complex Biological Membranes. *Proc. Natl. Acad. Sci.* 84, 429-433 (1987).
- Pierce, S.K. Lipid Rafts and B-cell Activation. *Nat. Rev. Immun.* 2, 96-105, doi: 10.1038/nri726 (2002).

- Radhakrishnan, A., Anderson, T.G., McConnell, H.M. Condensed Complexes, Rafts, and the Chemical Activity of Cholesterol in Membranes. *Proc. Natl. Acad. Sci.* 97, 23, 12422-12427, doi: 10.1073/pnas.220418097 (2000).
- Riff, J.D., Callahan, J.W., Sherman, P.M. Cholesterol-Enriched Membrane Microdomains Are Required for Inducing Host Cell Cytoskeleton Rearrangements in Response to Attaching-Effacing Escherichia coli. *Infect Immun.* 73, 11, 7113-7125, doi: 10.1128/IAI.73.11.7113-7125.2005 (2005).
- Rodionov, V.O., Fokin, V.V., Finn M.G.. Mechanism of the Ligand-Free Cu(I)-Catalyzed Azide-Alkyne Cycloaddition Reaction. *Angew. Chem. Int. Ed.* 44, 2210-2215, doi: 10.1002/anie.200461496 (2005).
- Rodionov, V.O., Presolski, S.I., Gardinier, S., Lim, Y.H., Finn, M.G. Benzimidazole and Related Ligands for Cu-Catalyzed Azide-Alkyne Cycloaddition. *J. Am. Chem. Soc.*, 129, 12696-12704, doi: 10.1021/ja072678l (2007).
- Rostovtsev, V.V., Green, L.G., Fokin, V.V., Sharpless, K.B. A Stepwise Huisgen Cycloaddition Process: Copper (I)-Catalyzed Regioselective Ligation of Azides and Terminal Alkynes. *Angew. Chem. Int. Ed.* 41, 2596-2599, doi: 10.1002/1521-3773(20020715)41:14<2596::AID-ANIE2596>3.0.CO;2-4 (2002).
- Ruckenstein, E., Nagarajan, R. Thermodynamics of Amphiphilic Aggregation into Micelles and Vesicles. *Micellization, Solubilization, and Microemulsions*, Vol. 1, Plenum Press: New York (1977).
- Russell, S., Olorio, J. Compartmentalization in T-Cell Signalling: Membrane Microdomains and Polarity Orchestrate Signalling and Morphology. *Immunol. Cell Biol.* 84, 107-113, doi: 10.1111/j.1440-1711.2005.01415.x (2006).
- Sleight, R.G. Intracellular Lipid Transport in Eukaryotes. *Ann. Rev. Physiol.* 49, 193-208, doi: 10.1146/annurev.ph.49.030187.001205 (1987).
- Simons, K., Vaz, W.L.C. Model Systems, Lipid Rafts, and Cell Membranes. *Annu. Rev. Biophys. Biomol. Struct.* 33, 269-295, doi: 10.1146/annurev.biophys.32.110601.141803 (2004).
- Sivakumar, K., Xie, F., Cash, B.M., Long, S., Barnhill, H.N., Wang, Q. A fluorogenic 1,3-dipolar cycloaddition reaction of 3-azidocoumarins and acetylenes. *Org. Lett.* 6, 4603-4606, doi:10.1021/ol047955x (2004).
- Smith, M.D. *et al.* Synthesis and Convenient Functionalization of Azide-Labeled Diacylglycerol Analogues for Modular Access to Biologically Active Lipid Probes. *Bioconjugate Chem.* 19, 9, 1855-1863, doi: 10.1021/bc/800102 (2008).
- Worrell, B.T., Malik, J.A., Fokin, V.V. Direct Evidence of a Dinuclear Copper Intermediate in Cu(I)-Catalyzed Azide-Alkyne Cycloadditions. *Science*, 340, 6131, 457-460, doi: 10.1126/science.1229506 (2013).
- Young, R.M., Holowka, D., Baird, B. A Lipid Raft Environment Enhances Lyn Kinase Activity by Protecting the Active Site Tyrosine from Dephosphorylation. *J. Bio. Chem.* 278, 20746-20752, doi: 10.1074/jbc.M211402200 (2003).